Supporting information for

Rational engineering of biomimetic flavylium fluorophores for regulating the lysosomal and mitochondrial localization behavior by pH-induced structure switch and application to fluorescence imaging

Liping Wang, Mengye He, Yu Sun, Li Liu, Yuan Ye, Lingrong Liu, Xing-can Shen, Hua Chen*

State Key Laboratory for Chemistry and Molecular Engineering of Medicinal Resources, Collaborative Innovation Center for Guangxi Ethnic Medicine, School of Chemistry and Pharmaceutical Science, Guangxi Normal University, Guilin, 541004, P. R. China.

*Email: chenhuagnu@gxnu.edu.cn (H. Chen)

Table of Contents

Pages

Materials and instruments. Unless otherwise stated, all reagents were purchased from commercial suppliers and used without further purification. Solvents used were purified by standard methods prior to use. Twice-distilled water was used throughout all experiments. Mass spectra were performed using an LCQ Advantage ion trap mass spectrometer from Thermo Finnigan or Agilent 1100 HPLC/MSD spectrometer. ^{1}H NMR and ^{13}C NMR spectra were recorded at ambient temperature using a Bruker AVANCE NEO 400 MHz and 600 MHz spectrometers, using TMS as an internal standard. Electronic absorption spectra were obtained on a Labtech UV Power PC spectrometer. Photoluminescent spectra were recorded at room temperature with a HITACHI F4600 fluorescence spectrophotometer with the excitation and emission slit widths at 10.0 and 10.0 nm respectively. The fluorescence imaging of cells was performed with Two-photon Confocal Scanning Laser Microscope (TCS SP8 DIVE). TLC analysis was performed on silica gel plates and column chromatography was conducted over silica gel (mesh 200-300), both of which were obtained from the Qingdao Ocean Chemicals.

Determination of the fluorescence quantum yield: Fluorescence quantum yields for the probes were determined by using Fluorescein (Φ_f = 0.79 in 0.1 M NaOH, for **FL-1**, **FL-2**), Rh6G (Φ_f =0.95 in EtOH, for **FL-5**) and cresol purple (Φ_f = 0.58 in ethanol, for other **FL** dyes) as a fluorescence standard. The quantum yield was calculated using the following equation:

$$\Phi_{F(X)} = \Phi_{F(S)} \, (A_S F_X / A_X F_S) \, (n_X / n_S)^2$$

Where Φ_F is the fluorescence quantum yield, A is the absorbance at the excitation wavelength, F is the area under the corrected emission curve, and n is the refractive index of the solvents used. Subscripts S and X refer to the standard and to the unknown, respectively.

Cytotoxicity azzssays. The toxicity of the probes towards living HeLa cells was determined by MTT (3-(4,5-dimethyl-2-thiazolyl)-2,5-diphenyl-2-H-tetrazolium bromide) assays. HeLa cells were grown in the Eagle's medium (1640) supplemented with 10% FBS (fetal bovine serum) in an atmosphere of 5% CO_2 and 95% air at 37 ºC. Immediately before the experiments, the cells were placed in a 96-well plate, followed

by addition of increasing concentrations of the probes (99%1640 and 1% DMSO). The final concentrations of the probes was 0, 5, 10, 15, 20, 25 μM (n = 5) respectively. The cells were then incubated at 37 ºC in an atmosphere of 5% CO_2 and 95% air at 37 ºC for 24 h, followed by MTT assays. Untreated assay with 1640 (n = 5) was also conducted under the same conditions.

HeLa cells, T24 cells and HL-7702 cells Culture and Imaging Using FL dyes.

T24 cells, HL-7702 cells were seeded in Dulbecco's modified Eagle'smedium (DMEM) supplemented with 10% fetal bovine serum for 24 h. HeLa cells were seeded in RPMI 1640 Media supplemented with 10% fetal bovine serum for 24 h. T24 cells, HL-7702 cells, and HeLa cells were incubated with 10.0 μM **FL** dyes for 30 min, and then treated with Lyso-Trackers Green, Lyso-Trackers Red, Mito-Trackers Green, or Mito-Trackers Deep Red for another 15 min. The fluorescence imaging of cells was performed with with Two-photon Confocal Scanning Laser Microscope (TCS SP8 DIVE). For **FL-1**: λ_{ex} = 488 nm, λ_{em} = 498-550 nm; For **FL-2**: λ_{ex} = 488 nm, λ_{em} = 498-550 nm; For **FL-3**: λ_{ex} = 552 nm, λ_{em} = 562-610 nm; For **FL-4**: λ_{ex} = 638 nm, λ_{em} = 650-750 nm; For **FL-5**: λ_{ex} = 488 nm, λ_{em} = 498-550 nm; For **FL-6**: λ_{ex} = 552 nm, λ_{em} = 562-610 nm; For **FL-7**: λ_{ex} = 552 nm, λ_{em} = 562-650 nm; For **FL-8**: λ_{ex} = 638 nm, λ_{em} = 650-750 nm; For **FL-9**: λ_{ex} = 638 nm, λ_{em} = 650-780 nm; For Lyso-Tracher Green: λ_{ex} = 488 nm, λ_{em} = 498-550 nm; For Lyso-Tracher Red: λ_{ex} = 552 nm, λ_{em} = 580-610 nm; For Mito-Tracher Green: λ_{ex} = 488 nm, λ_{em} = 498-550 nm; For Mito-Tracher Deep Red: λ_{ex} = 638 nm, λ_{em} = 650-700 nm.

Fluorescent imaging in living mice using probe FL-9.

Female BALB/C mice aged about 5 weeks were purchased from Hunan Slack Jingda Experimental Animal Co., Ltd. The tumors were developed by subcutaneously implanting 4×10^6 4T1 cells into the left hind leg injections of female BALB/c mice. Tumor volume was calculated using the following formula: volume = (tumor length)×(tumor width)^2 /2. When the tumor volume reached 200 mm^3, the mice were administered with **FL-9** (20 μM). After the probe post-injection, the mice were imaged using a Kodak in vivo FX Pro imaging system (Bruker). With an excitation filter of 650 nm and the emission filter of 700 nm.

Synthesis of compound B1.

$POC1_3$ (2.0 mL) was added dropwisely by a separatory funnel to a flask containing DMF (5 mL) with stirring at 0 ℃ over 30 min. Subsequently, compounds **A1** (1 g) in DMF (0.5 mL) was added slowly with stirring and the mixture was heated for 5 h at 60 °C. Then the mixture was poured to ice water and the resulting precipitate was filtered off and washed with cold water (200 mL) to afford the light yellow solid **B1**, which was utilized in the next reaction without purification again. ^{1}H NMR (400 MHz, $CDCl_3$) δ 10.39 (s, 1H), 7.87 (d, *J* = 7.5 Hz, 1H), 7.39 -7.32 (m, 2H), 7.22 (d, *J* = 7.1 Hz, 1H), 2.85 (t, *J* = 8.0 Hz, 2H), 2.64 (t, *J* = 8.0 Hz, 2H). ^{13}C NMR (100 MHz, $CDCl_3$) δ 190.71, 145.91, 138.99, 132.03, 131.41, 127.74, 127.11, 126.34, 27.04, 21.60.

Synthesis of compound B2.

$POC1_3$ (2.0 mL) was added dropwisely by a separatory funnel to a flask containing DMF (5 mL) with stirring at 0 ℃ over 30 min. Subsequently, compounds **A2** (1 g) in DMF (0.5 mL) was added slowly with stirring and the mixture was heated for 5 h at 60 °C. Then the mixture was poured to ice water and the resulting precipitate was filtered off and washed with cold water (200 mL) to afford the light yellow solid **B2**,

which was utilized in the next reaction without purification again. ^{1}H NMR (400 MHz, $CDCl_3$) δ 10.33 (s, 1H), 7.80 (d, *J* = 8.7 Hz, 1H), 6.84 (dd, *J* = 8.7, 1.9 Hz, 1H), 6.75 (s, 1H), 3.86 (s, 3H), 2.82 (t, *J* = 7.9 Hz, 2H), 2.63 (t, *J* = 7.9 Hz, 2H). ^{13}C NMR (100 MHz, $CDCl_3$) δ 190.46, 162.19, 146.09, 141.31, 129.82, 128.37, 124.90, 113.56, 112.11, 55.49, 27.58, 21.54.

Synthesis of compound B3.

$POC1_3$ (2.0 mL) was added dropwisely by a separatory funnel to a flask containing DMF (5 mL) with stirring at 0 ℃ over 30 min. Subsequently, compounds **A3** (1 g) in DMF (0.5 mL) was added slowly with stirring and the mixture was heated for 5 h at 60 °C. Then the mixture was poured to ice water and the resulting precipitate was filtered off and washed with cold water (200 mL) to afford the light yellow solid **B3**, which was utilized in the next reaction without purification again. ^{1}H NMR (400 MHz, $CDCl_3$) δ 10.27 (s, 1H), 7.72 (d, *J* = 8.8 Hz, 1H), 6.60 (d, *J* = 8.8 Hz, 1H), 6.49 (s, 1H), 3.06 (s, 6H), 2.79 (t, *J* = 7.9 Hz, 2H), 2.62 (t, *J* = 7.9 Hz, 2H). ^{13}C NMR (100 MHz, $CDCl_3$) δ 190.15, 141.19, 128.30, 110.51, 109.90, 40.15, 28.22, 21.76.

General procedure for synthesis of FL1-9.

Compound **A** (0.5 mmol) and **B** (0.5 mmol) were dissolved with a mixture of AcOH (8 mL) and $HClO_4$ (2 mL). After refluxing and stirring for 4 h, the mixture was poured into ice water (200 mL), and then the aqueous phase was extracted with dichloromethane (3 × 100 mL). The organic layers were collected and evaporated under reduced pressure. Finally, the crude products were purified by column chromatography on silica gel flash chromatography to give compounds **FL1-9**.

Synthesis of compound FL-1

Yellow solid; yield 62.9%; ^{1}H NMR (400 MHz, DMSO-d_6) δ 8.83 (s, 1H), 8.38 (d, *J* = 7.8 Hz, 2H), 7.73 (t, *J* = 7.5 Hz, 2H), 7.65-7.53 (m, 4H), 3.21-3.14 (m, 8H). ^{13}C

NMR (100 MHz, DMSO-d_6) δ 165.42, 153.99, 142.38, 135.61, 132.06, 129.72, 128.82, 126.56, 125.92, 25.95, 25.32. HRMS (ESI) Calcd for $C_{21}H_{17}O^+$ ([M]$^+$): 285.1274, Found, 285.1274.

Synthesis of compound FL-2

Yellow solid; yield 65.1%; ^{1}H NMR (400 MHz, DMSO-d_6) δ 8.68 (s, 1H), 8.34 (dd, *J* = 16.9, 8.2 Hz, 2H), 7.69 (t, *J* = 7.3 Hz, 1H), 7.61-7.51 (m, 2H), 7.15 (d, *J* = 7.9 Hz, 2H), 3.95 (s, 3H), 3.18 -3.07 (m, 8H). ^{13}C NMR (100 MHz, DMSO-d_6) δ 166.19, 165.74 , 163.47, 152.59 , 146.05 , 141.65 , 134.92 , 130.99 , 130.00 , 129.58 , 129.37 , 128.65 , 126.03 , 126.00, 118.63 , 115.60 , 114.55 , 56.64 , 26.62 , 26.21 , 25.42 , 25.12. HRMS (ESI) Calcd for $C_{22}H_{19}O_2^+$ ([M]$^+$): 315.1380, Found, 315.1372.

Synthesis of compound FL-3

Yellow solid; yield 63.2%; ^{1}H NMR (400 MHz, DMSO-d_6) δ 8.22 (s, 1H), 8.13 (d, *J* = 3.4 Hz, 1H), 7.58 (t, *J* = 7.3 Hz, 1H), 7.51 (t, *J* = 7.4 Hz, 1H), 7.46 -7.41 (m, 2H), 6.80-6.69 (m, 1H), 6.56 (d, *J* = 6.7 Hz, 1H), 3.06-2.91 (m, 8H). ^{13}C NMR (100 MHz, DMSO-d_6) δ 166.62, 158.89, 157.90, 147.84, 147.06, 140.13, 133.38, 130.54, 129.96, 129.27, 128.32, 126.43, 125.50, 124.68, 115.04, 112.70, 26.87, 26.39, 25.83, 24.78. HRMS (ESI) Calcd for $C_{21}H_{18}NO^+$ ([M]$^+$): 300.1383, Found, 300.1379.

Synthesis of compound FL-4

Red solid; yield 68.8%; ^{1}H NMR (400 MHz, DMSO-d_6) δ 8.25 (s, 1H), 8.15 (d, *J* =4.4 Hz, 1H), 7.73-7.65 (m, 1H), 7.61-7.51 (m, 2H), 7.46 (d, *J* = 7.3 Hz, 1H), 6.92 (dd, *J* = 9.1, 2.3 Hz, 1H), 6.84 -6.72 (m, 1H), 3.20 (s, 6H), 3.06-3.00 (m, 8H). ^{13}C NMR (100 MHz, DMSO-d_6) δ 166.58, 159.30, 155.82, 148.06, 146.12, 140.26, 133.50, 132.00, 130.24, 129.62, 129.23, 128.39, 126.45, 125.92, 124.75, 112.92, 111.29, 65.50, 30.48, 27.11, 26.39, 24.83. HRMS (ESI) Calcd for $C_{23}H_{22}NO^+$ ([M]$^+$): 328.1696, Found, 328.1690.

Synthesis of compound FL-5

Yellow solid; yield 65.7%; ^{1}H NMR (400 MHz, DMSO-d_6) δ 8.55 (s, 1H), 8.25 (d, J = 9.0 Hz, 2H), 7.10 (d, J = 7.5 Hz, 4H), 3.92 (s, 6H), 3.08 (s, 8H). ^{13}C NMR (400 MHz, DMSO-d_6) δ 165.15, 164.43, 151.66, 145.19, 128.94, 128.69, 118.69, 115.25, 114.51, 56.51, 26.65, 25.21. HRMS (ESI) Calcd for $C_{23}H_{21}O_3^+$ ([M]$^+$): 345.1485, Found, 345.1479.

Synthesis of compound FL-6

Red solid; yield 61.8%; ^{1}H NMR (400 MHz, DMSO-d_6) δ 8.19 (s, 1H), 8.11 (d, J = 8.4 Hz, 1H), 8.05 (d, J = 8.8 Hz, 1H), 7.22 (s, 1H), 7.06 (s, 1H), 6.73 (dd, J = 8.8, 2.0 Hz, 1H), 6.55 (s, 1H), 3.89 (s, 3H), 3.02-2.89 (m, 8H). ^{13}C NMR (400 MHz, DMSO-d_6) δ 165.72, 163.89, 157.28, 148.03, 146.26, 143.41, 129.87, 128.09, 127.19, 124.51, 119.13, 114.68, 114.60, 114.43, 112.75, 56.30, 29.48, 26.93, 26.83, 25.66, 24.89. HRMS (ESI) Calcd for $C_{22}H_{20}NO_2^+$ ([M]$^+$): 330.1489, Found, 330.1488.

Synthesis of compound FL-7

Red solid; yield 66.2%; ^{1}H NMR (400 MHz, DMSO-d_6) δ 8.22 (s, 1H), 8.11 (d, J = 4.1 Hz, 1H), 7.72 (dt, J = 6.9, 3.6 Hz, 1H), 7.66 (dd, J = 5.8, 3.2 Hz, 1H), 7.09-7.04 (m, 2H), 6.77 (d, J = 2.2 Hz, 1H), 3.90 (s, 3H), 3.18 (s, 6H), 3.04 -2.96 (m, 8H). ^{13}C NMR (100 MHz, DMSO-d_6) δ 166.56, 159.28, 155.80, 148.04, 146.10, 140.25, 133.49, 131.99, 130.22, 129.60, 129.22, 128.38 (s), 126.43, 125.91, 124.74, 112.91, 111.28, 65.49, 27.11, 26.39, 25.89, 24.83. HRMS (ESI) Calcd for $C_{24}H_{24}NO_2^+$ ([M]$^+$): 358.1802, Found, 358.1796.

Synthesis of compound FL-8

Purple solid; yield 69.3%; ^{1}H NMR (400 MHz, DMSO-d_6) δ 8.04 (s, 1H), 7.99 (d, J = 9.0 Hz, 1H), 7.92 (d, J = 8.7 Hz, 1H), 6.88 (s, 1H), 6.81 (dd, J = 9.0, 2.5 Hz, 1H), 6.73-6.70 (m, 1H), 6.53 (d, J = 2.0 Hz, 1H), 3.12 (s, 6H), 2.97-2.85 (m, 8H). ^{13}C NMR (400 MHz, DMSO-d_6) δ 163.26, 162.64, 155.94, 154.39, 147.01, 144.62,

143.67, 128.42, 127.55, 124.55, 124.30, 114.04, 113.17, 112.78, 111.84, 111.21, 31.62, 30.30, 27.32, 27.06, 25.36. HRMS (ESI) Calcd for $C_{23}H_{23}N_2O^+$ ($[M]^+$): 343.1805, Found, 343.1802.

Synthesis of compound FL-9

Purple solid; yield 70.4%; ^{1}H NMR (400 MHz, DMSO-d_6) δ 8.05 (s, 1H), 7.97 (d, J = 8.9 Hz, 2H), 6.83 (d, J = 8.4 Hz, 2H), 6.73 (s, 2H), 3.13 (s, 12H), 2.94 (s, 8H). ^{13}C NMR (400 MHz, DMSO-d_6) δ 162.94, 154.48, 147.01, 143.84, 127.62, 124.74, 113.13, 111.97, 111.21, 27.30, 25.40. HRMS (ESI) Calcd for $C_{25}H_{27}N_2O^+$ ($[M]^+$): 371.2118, Found, 371.2130.

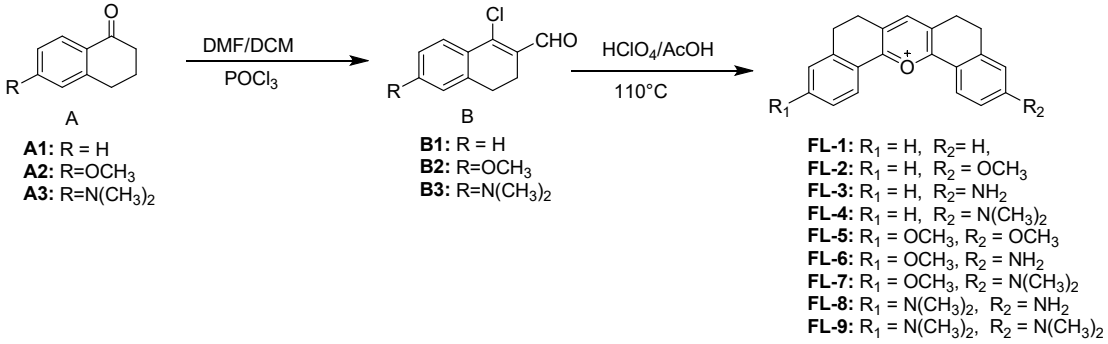

Scheme S1 Synthesis of flavylium fluorophores **FL-1~9**.

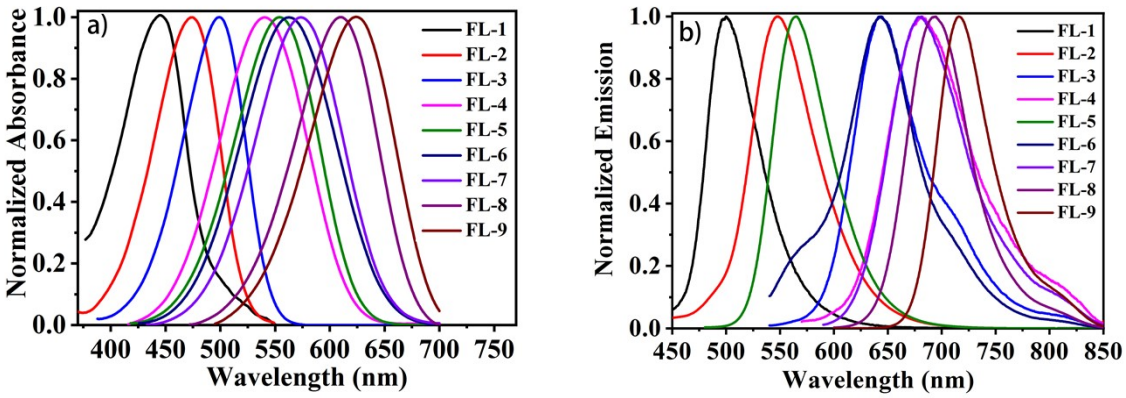

Figure S1 Normalized absorption (a) and fluorescence emission (b) spectra of 10 μM compounds **FL-1~9** in DMF.

Table S1 Photophysical properties of the compounds **FL-1~9** in DMF.

Compound	λ_{abs} (nm)	ε_{max} ($10^4 M^{-1} cm^{-1}$)	E_x (nm)	λ_{em} (nm)	Φ_f	Stokes Shift (nm)
FL-1	445	0.25	432	500	0.14	55
FL-2	475	0.99	476	550	0.36	75
FL-3	542	0.78	556	643	0.02	101
FL-4	563	0.53	583	682	0.02	119
FL-5	499	0.27	489	566	0.53	67
FL-6	554	1.89	556	643	0.06	89
FL-7	574	0.96	580	681	0.03	107
FL-8	610	0.32	600	693	0.02	83
FL-9	624	1.40	630	717	0.02	93

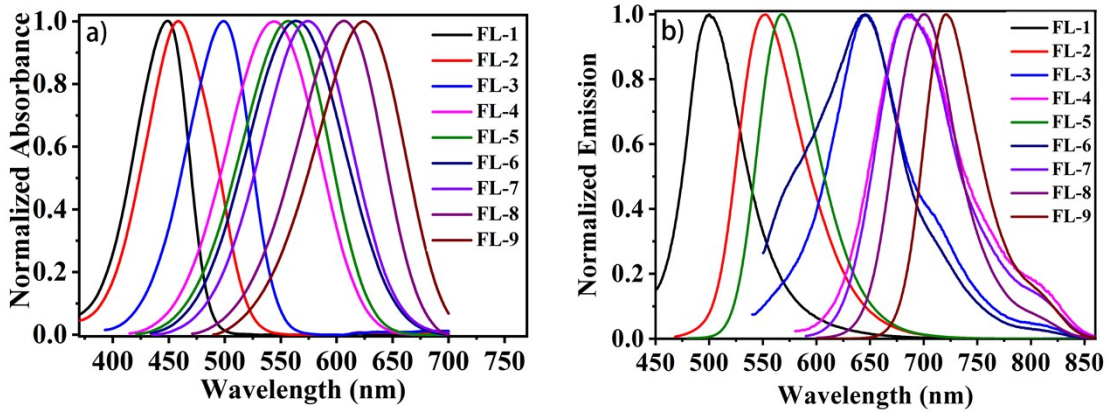

Figure S2 Normalized absorption (a) and fluorescence emission (b) spectra of 10 μM compounds **FL-1~9** in DMSO.

Table S2. Photophysical properties of the compounds **FL-1~9** in DMSO.

Compound	λ_{abs} (nm)	ε_{max} ($10^4 M^{-1} cm^{-1}$)	E_x (nm)	λ_{em} (nm)	Φ_f	Stokes Shift (nm)
FL-1	449	2.39	445	502	0.04	53
FL-2	459	1.44	456	552	0.06	93
FL-3	544	1.07	543	645	0.02	101
FL-4	564	1.66	560	686	0.01	122
FL-5	499	0.31	492	569	0.51	70
FL-6	557	1.89	534	645	0.05	88
FL-7	575	1.01	573	686	0.02	111
FL-8	607	0.52	598	702	0.01	95
FL-9	625	1.91	630	721	0.02	96

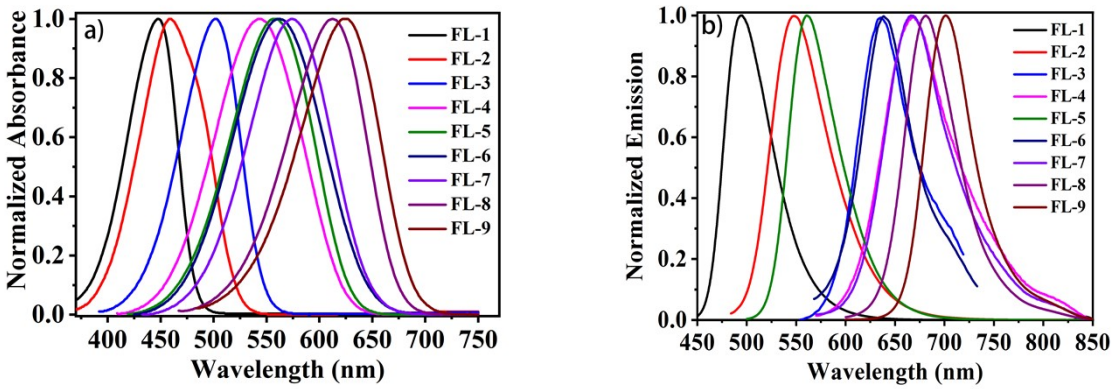

Figure S3 Normalized absorption (a) and fluorescence emission (b) spectra of 10 μM compounds **FL-1~9** in EtOH.

Table S3. Photophysical properties of the compounds **FL-1~9** in EtOH.

Compound	λ_{abs} (nm)	ε_{max} ($10^4 M^{-1} cm^{-1}$)	E_x (nm)	λ_{em} (nm)	Φ_f	Stokes Shift (nm)
FL-1	448	0.73	443	495	0.99	47
FL-2	459	1.30	455	547	0.73	88
FL-3	544	1.04	546	636	0.01	92
FL-4	561	1.61	576	667	0.02	106
FL-5	502	4.17	482	561	0.07	59
FL-6	558	2.01	550	640	0.08	82
FL-7	575	0.93	573	667	0.05	92
FL-8	613	0.57	580	683	0.04	70
FL-9	624	2.06	600	702	0.04	78

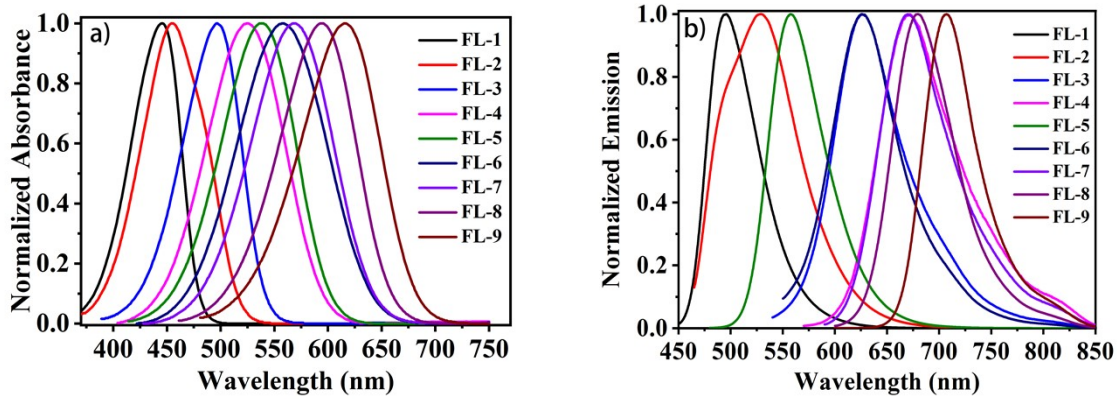

Figure S4 Normalized absorption (a) and fluorescence emission (b) spectra of 10 μM compounds **FL-1~9** in MeCN.

Table S4 Photophysical properties of the compounds **FL-1~9** in MeCN.

Compound	λ_{abs} (nm)	ε_{max} ($10^4 M^{-1} cm^{-1}$)	E_x (nm)	λ_{em} (nm)	Φ_f	Stokes Shift (nm)
FL-1	445	2.48	443	495	0.99	50
FL-2	456	1.11	446	528	0.89	72
FL-3	525	0.93	520	627	0.06	102
FL-4	559	1.44	555	671	0.02	112
FL-5	497	0.24	485	558	0.68	61
FL-6	538	1.86	532	627	0.02	89
FL-7	568	0.97	582	671	0.05	103
FL-8	594	0.51	600	681	0.03	87
FL-9	617	1.62	630	708	0.04	91

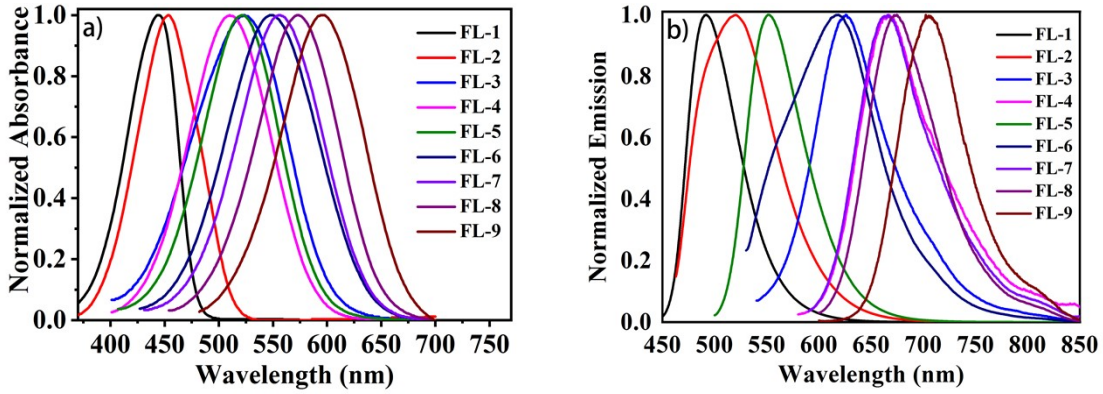

Figure S5 Normalized absorption (a) and fluorescence emission (b) spectra of 10 μM compounds **FL-1~9** in PBS.

Table S5 Photophysical properties of the compounds **FL-1~9** in PBS.

Compound	λ_{abs} (nm)	ε_{max} ($10^4 M^{-1} cm^{-1}$)	E_x (nm)	λ_{em} (nm)	Φ_f	Stokes Shift (nm)
FL-1	444	0.31	435	492	0.99	48
FL-2	453	1.04	452	520	0.83	67
FL-3	523	0.91	523	627	0.02	104
FL-4	549	1.02	546	664	0.01	115
FL-5	510	0.29	489	552	0.73	42

FL-6	523	1.75	522	618	0.02	95
FL-7	557	1.75	556	664	0.01	107
FL-8	574	0.41	586	673	0.01	99
FL-9	596	1.46	615	705	0.05	109

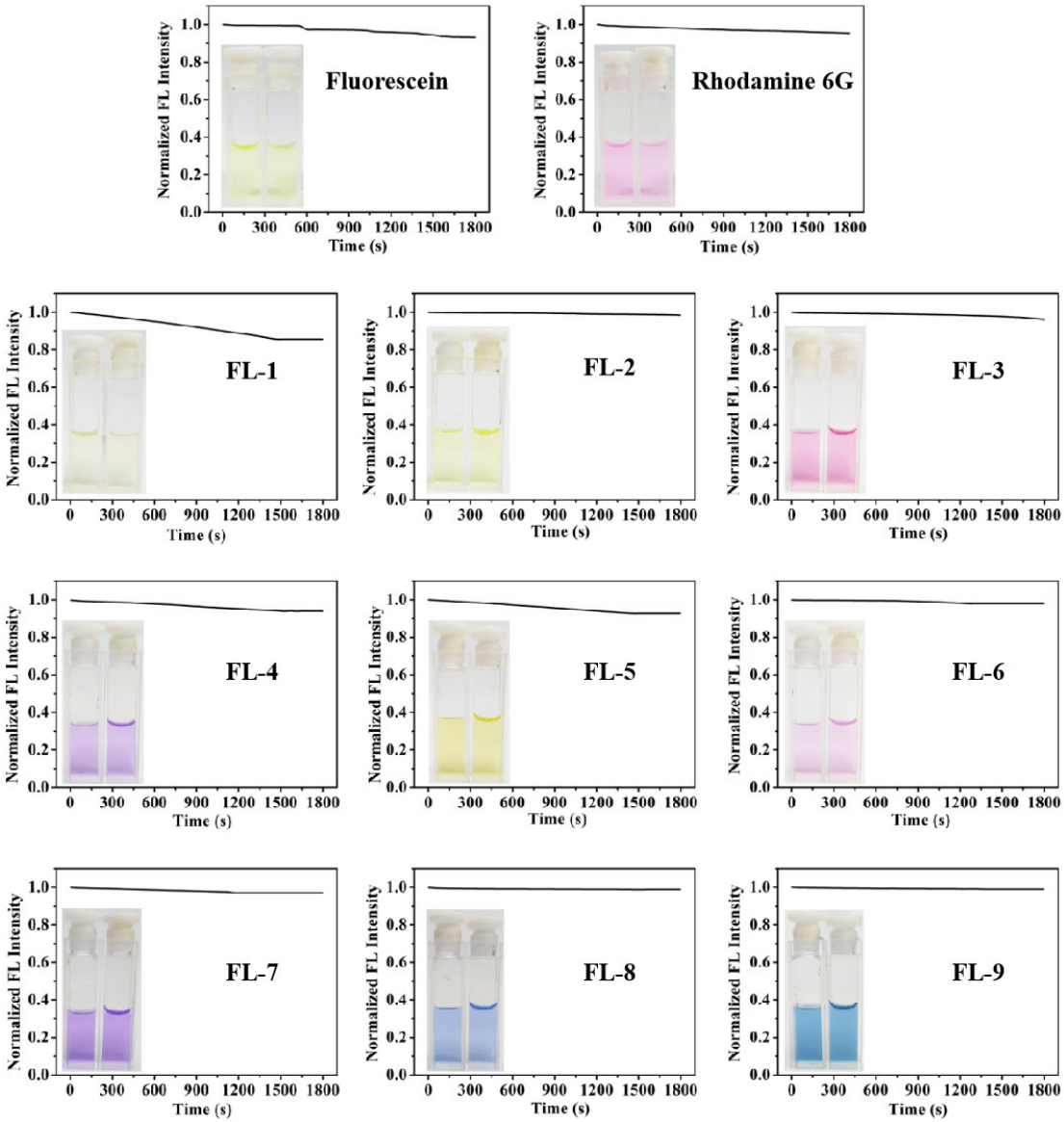

Figure S6 Photostability test of the **FL-1~9** by Xenon lamp (150 W) irradiation within 30 min (normalized fluorescence intensity vs. time). The excitation wavelengths of the spectra obtained for dyes **FL-1~9** refer to the wavelengths in PBS and emission wavelengths of the spectra obtained for dyes FL-1~9 also refer to the wavelengths in PBS. Insets: Color map of representative **FL** dyes before and after irradiation.

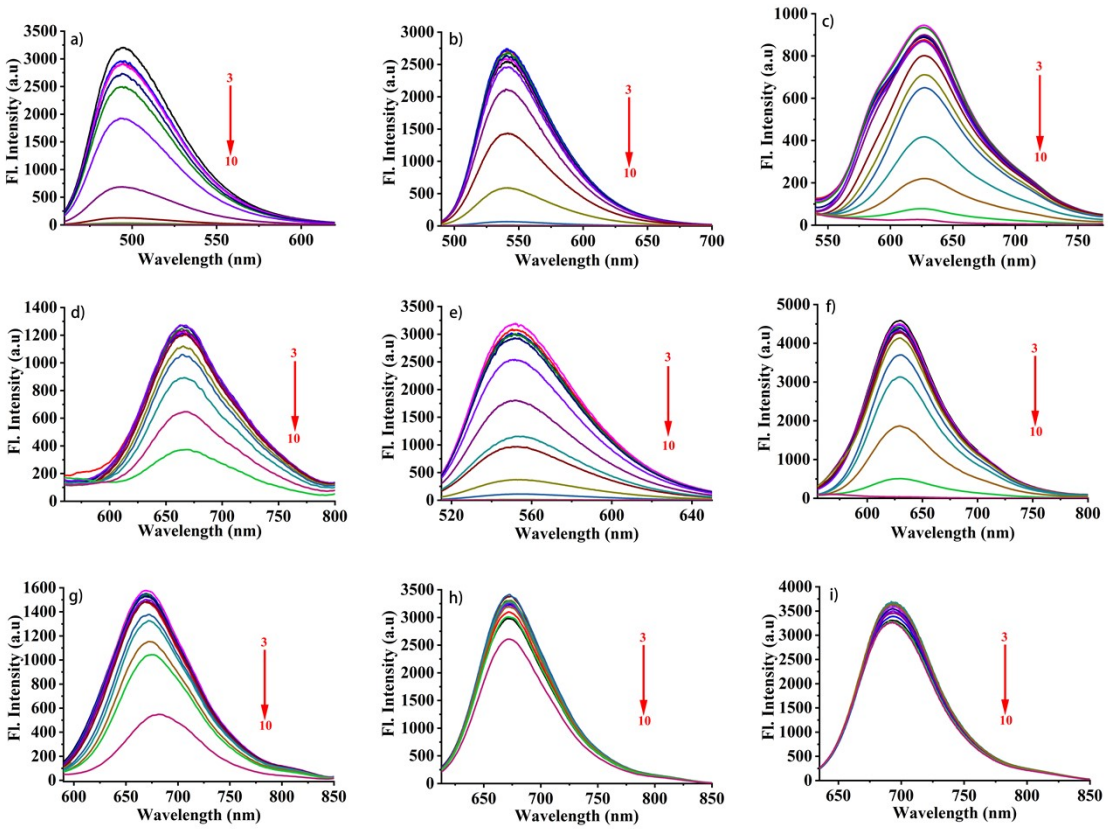

Figure S7 (a-i) pH-dependence of the fluorescence intensity of compounds **FL-1~9** (10 μM) with the arrow indicating the change of the fluorescence intensities with pH increase from 3 to 10.

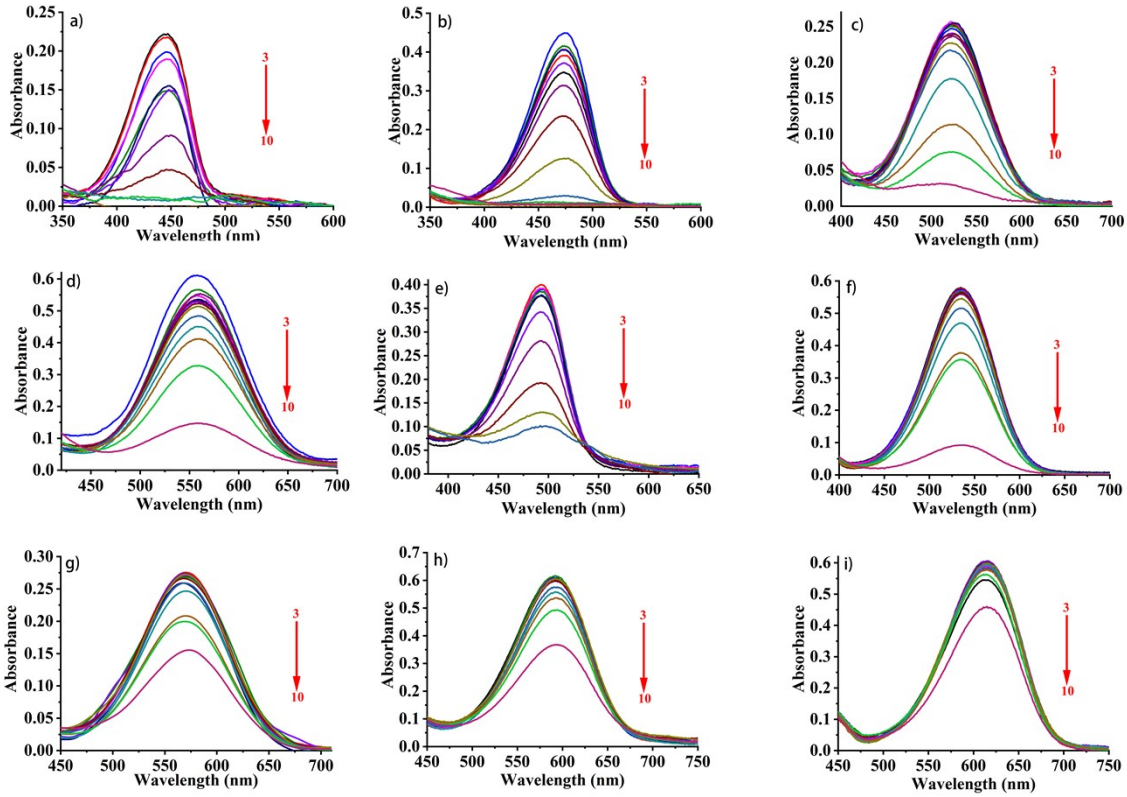

Figure S8 (a-i) pH-dependence of the UV of compounds **FL-1~9** (10 μM) with the arrow indicating the change of the UV absorbance with pH increase from 3 to 10.

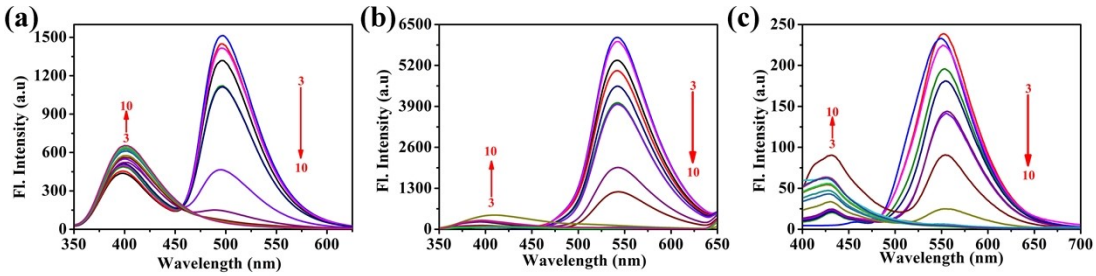

Figure S9 (a-c) pH-dependence of the fluorescence intensity of compounds **FL-1**, **FL-2**, **FL-5** (10 μM) with the arrow indicating the change of the fluorescence intensities with pH increase from 3 to 10. **FL-1** and **FL-2** (λ_{ex}=330 nm); **FL-5** (λ_{ex}=380 nm).

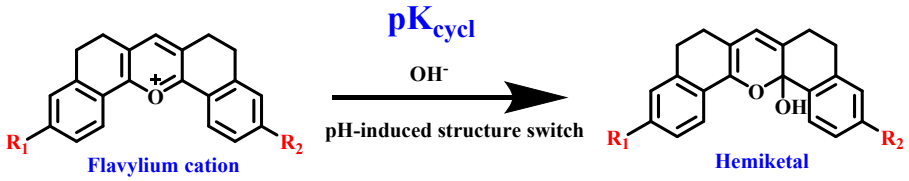

Scheme S2 pH-induced structure switch from flavylium cations to hemiketals of **FL**.

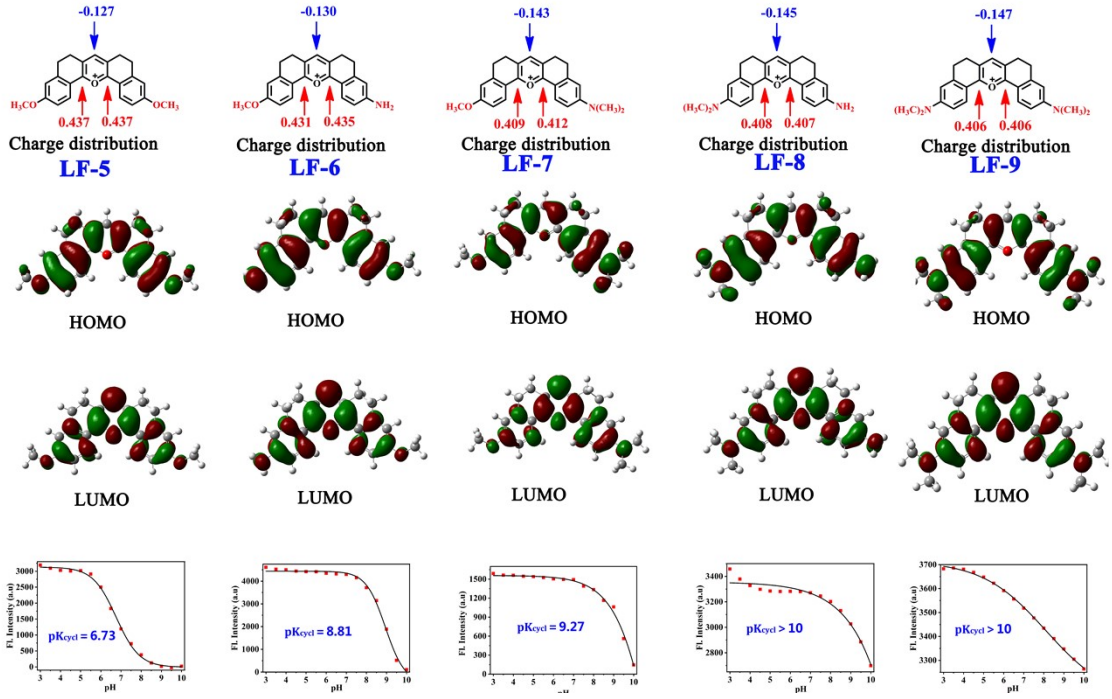

Figure S10 Charge distributions of flavylium rings, molecular orbital plots (LUMO and HOMO) of flavylium fluorophores and their corresponding pK$_{cycl}$ values.

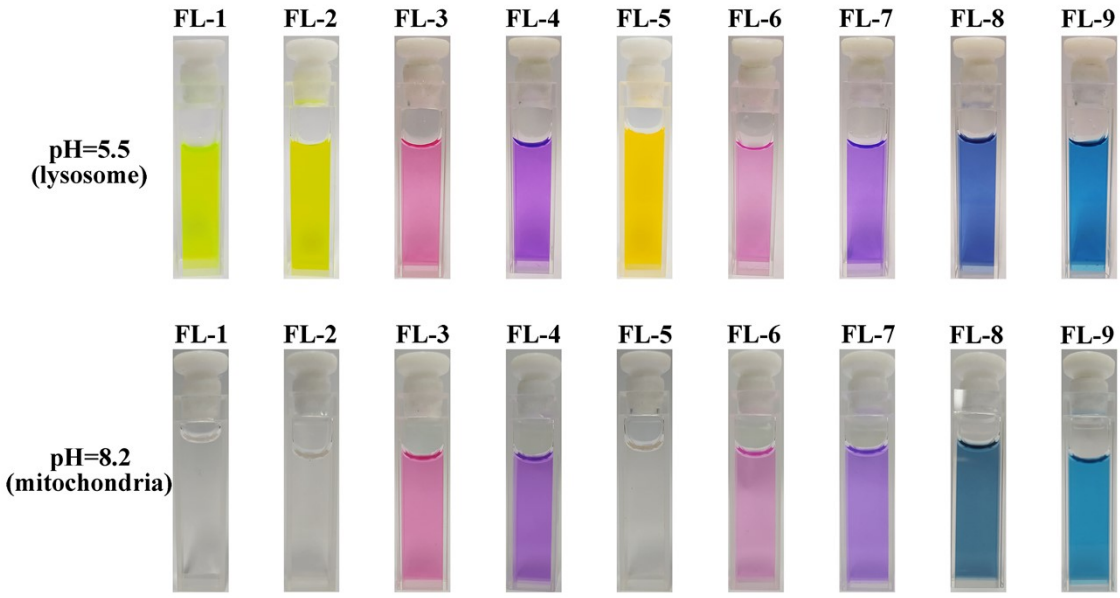

Figure S11 Color map of representative **FL** dyes that mimic lysosome and mitochondrial pH at the test-tube level.

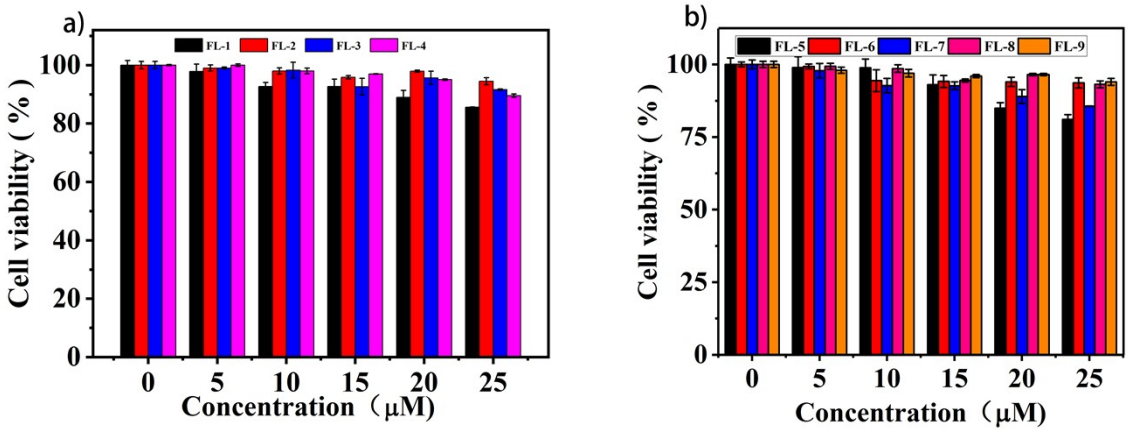

Figure S12 Cytotoxicity of **FL** dyes against HeLa cells.

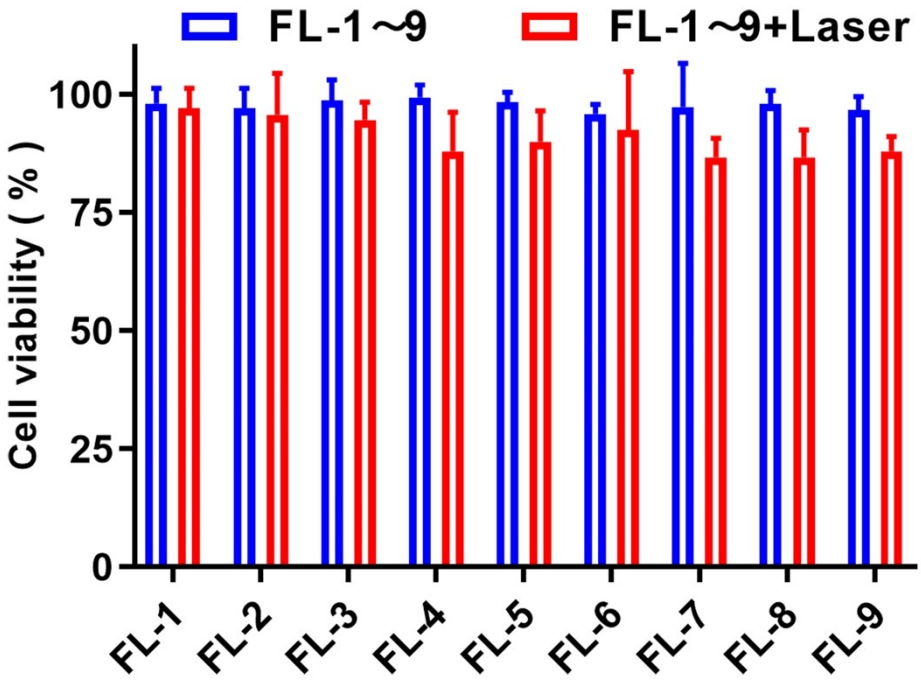

Figure S13 Cell viability of HeLa cells incubated with **FL** dyes (10μM) with or without laser irradiation (1.0 W cm^{-2}).

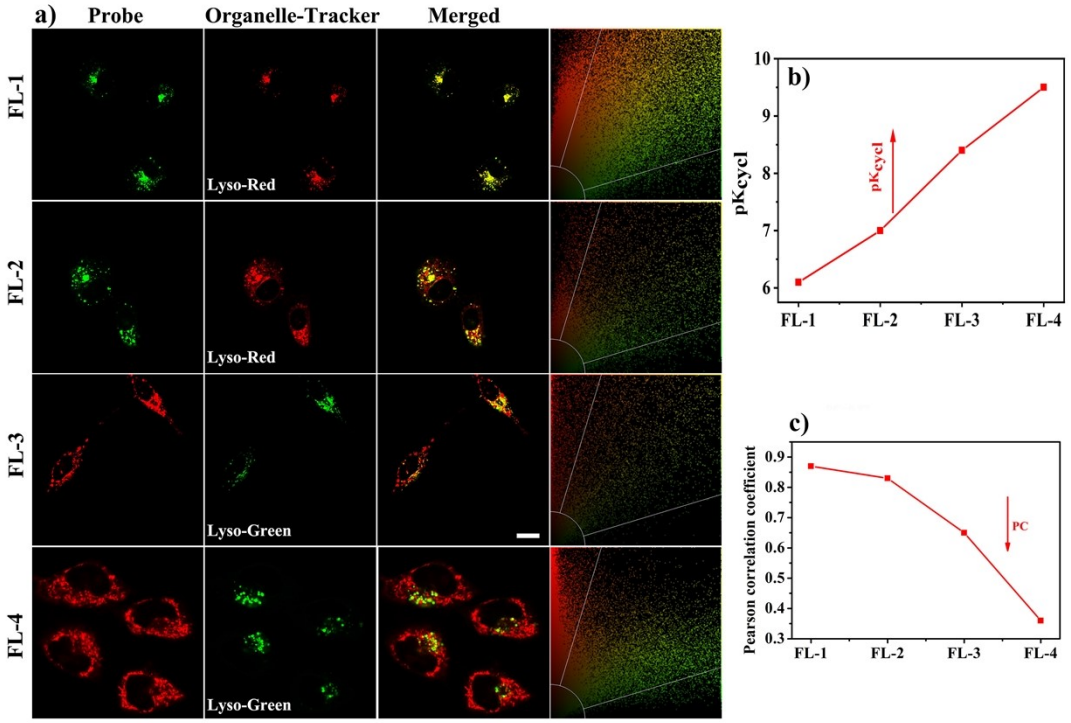

Figure S14 Confocal fluorescence images of **FL-1~4** dyes by HL-7702 cells via TCS SP8 DIVE imaging. (a) HL-7702 cells were co-stained with **FL-1~4** dyes and

different Lyso Trackers; (b) The pK_{cycl} value of **FL-1~4** dyes; (c) The Pearson's correlation coefficient of **FL-1~4** dyes. All images were obtained at 63 oil magnification. Confocal fluorescence images of **FL-1** (λ_{ex} = 488 nm, λ_{em} = 498-550 nm); **FL-2** (λ_{ex} = 488 nm, λ_{em} = 498-550 nm); **FL-3** (λ_{ex} = 552 nm, λ_{em} = 562-610 nm); **FL-4** (λ_{ex} = 638 nm, λ_{em} = 650-750 nm); Lyso-Tracher Red (λ_{ex} = 552 nm, λ_{em} = 580-610 nm); Lyso-Tracher Green (λ_{ex} = 488 nm, λ_{em} = 500-550 nm). Scale bar=10 μm.

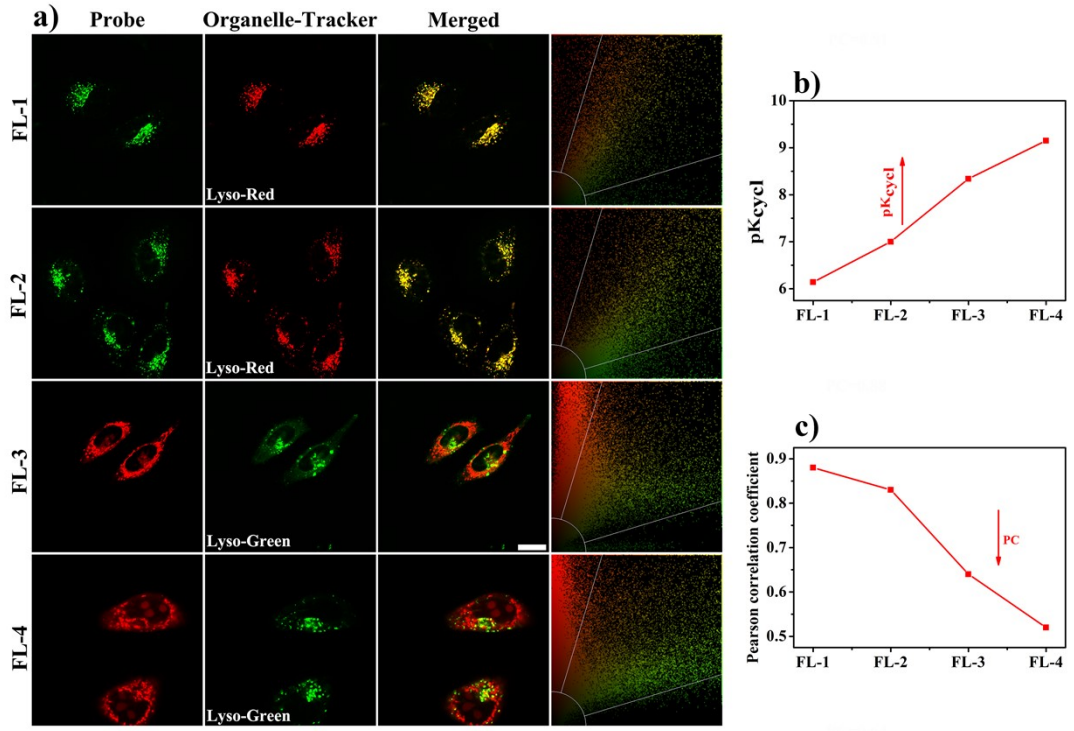

Figure S15 Confocal fluorescence images of **FL-1~4** dyes by T24 cells via TCS SP8 DIVE imaging. (a) T24 cells were co-stained with **FL-1~4** dyes and different Lyso Trackers; (b) The pK_{cycl} value of **FL-1~4** dyes; (c) The Pearson's correlation coefficient of **FL-1~4** dyes. All images were obtained at 63 oil magnification. Confocal fluorescence images of **FL-1** (λ_{ex} = 488 nm, λ_{em} = 498-550 nm); **FL-2** (λ_{ex} = 488 nm, λ_{em} = 498-550 nm); **FL-3** (λ_{ex} = 552 nm, λ_{em} = 562-610 nm); **FL-4** (λ_{ex} = 638 nm, λ_{em} = 650-750 nm); Lyso-Tracher Red (λ_{ex} = 552 nm, λ_{em} = 580-610 nm); Lyso-Tracher Green (λ_{ex} = 488 nm, λ_{em} = 500-550 nm). Scale bar=10 μm.

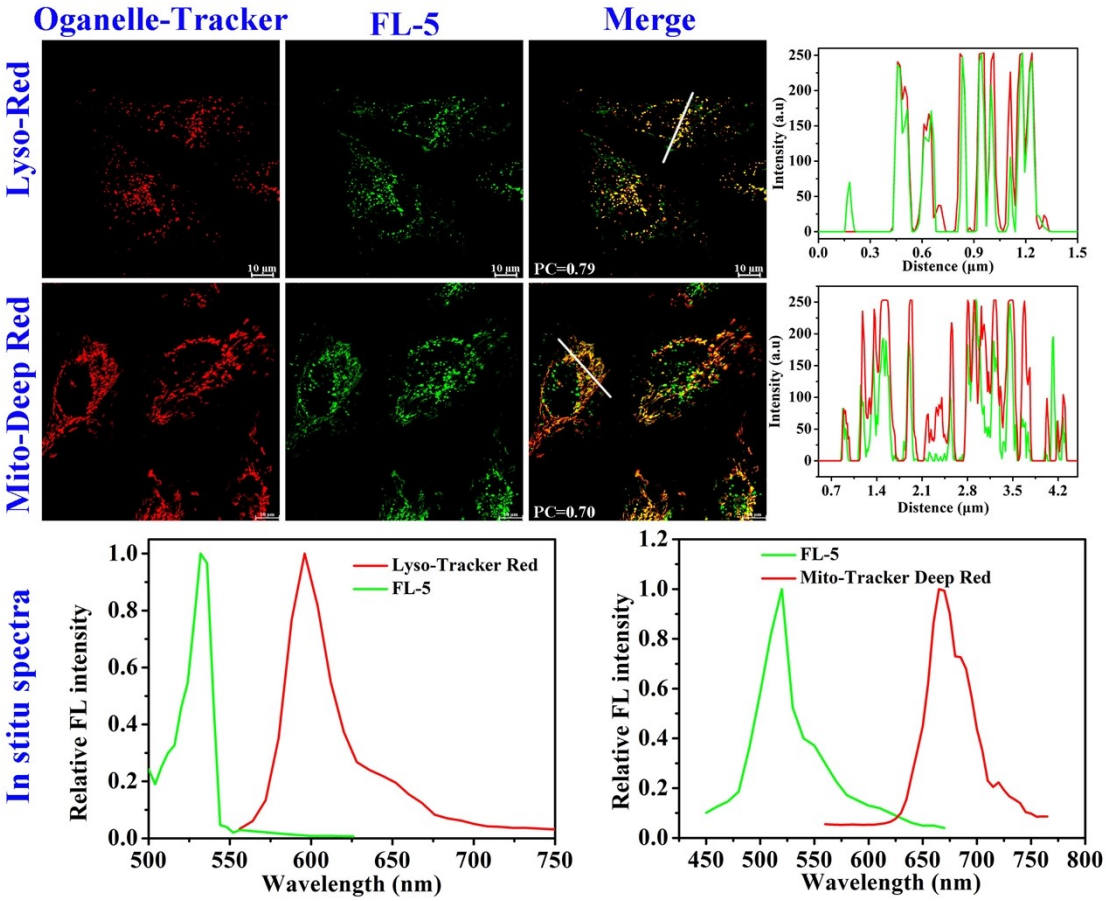

Figure S16 Confocal fluorescence images of **FL-5** dyes and different organelle trackers by HeLa cells via TCS SP8 DIVE imaging, as well as the corresponding in situ spectra in **FL-5** and different organelle trackers. For **FL-5:** λ_{ex} = 488 nm, λ_{em} = 498-550 nm; For Lyso-Tracher Red: λ_{ex} = 552 nm, λ_{em} = 580-610 nm; For Mito-Tracher Deep Red: λ_{ex} = 638 nm, λ_{em} = 650-750 nm. Scale bar=10 μm.

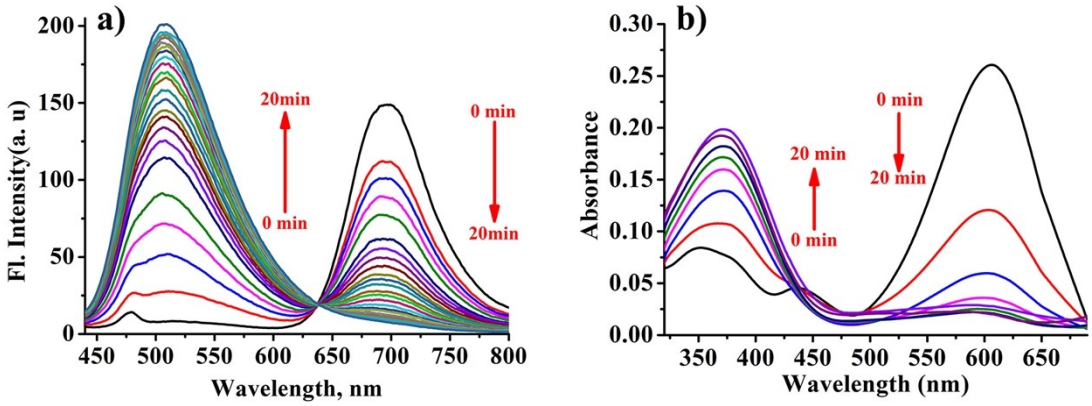

Figure S17 Time-dependent fluorescence and absorption spectra of probe **FL-9** (10 μM) in the presence of 100 μM Na_2S in PBS buffer (pH=7.4). Excitation, 410 nm.

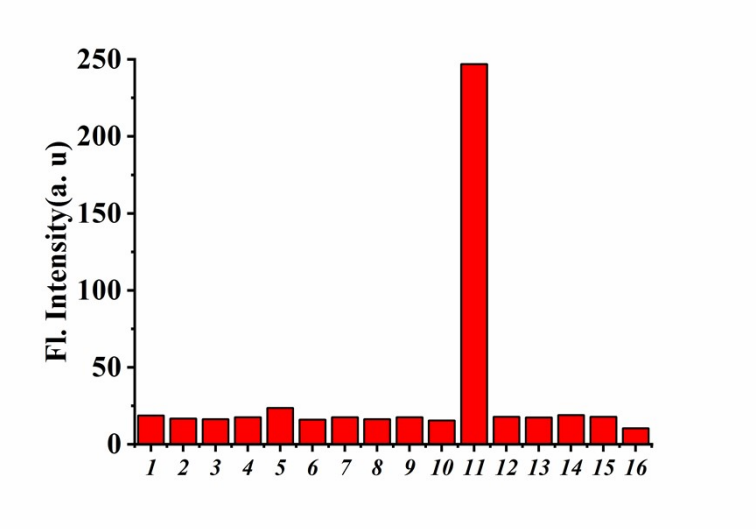

Figure S18 The fluorescence enhancement at 506 nm to various biologically relevant species in aqueous solution (pH 7.4, 25 mM PBS with 20% DMSO). 1. Blank, 2. HSO_3^- (25 μM), 3. CN^-(25 μM), 4. CO_3^{2-}(25 μM), 5. N_3^-(25 μM), 6. NO_2^-(25 μM), 7. $H_2PO_4^-$(25 μM), 8. NO_3^-(25 μM), 9. SO_4^{2-}(25 μM), 10. SCN^-(25 μM), 11. Na_2S(25 μM), 12. $S_2O_3^{2-}$(25 μM), 13. Cys(1 mM), 14. GSH(1 mM), 15. I^-(25 μM), 16. Cl^-(25 μM). Excitation, 410 nm.

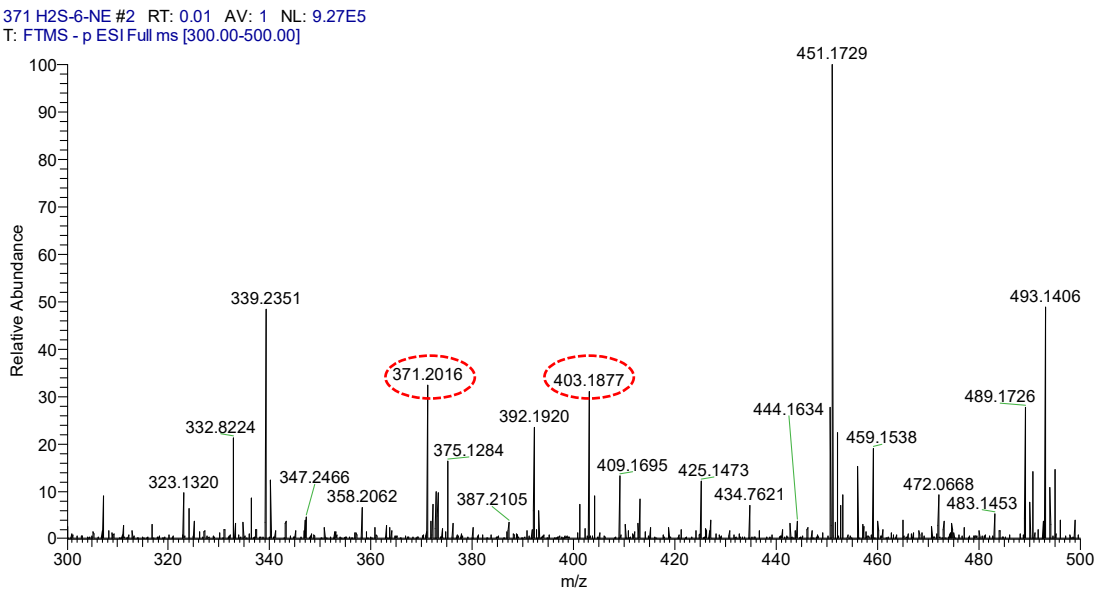

Figure S19 The HRMS of the probe **FL-9** upon addition of Na_2S.

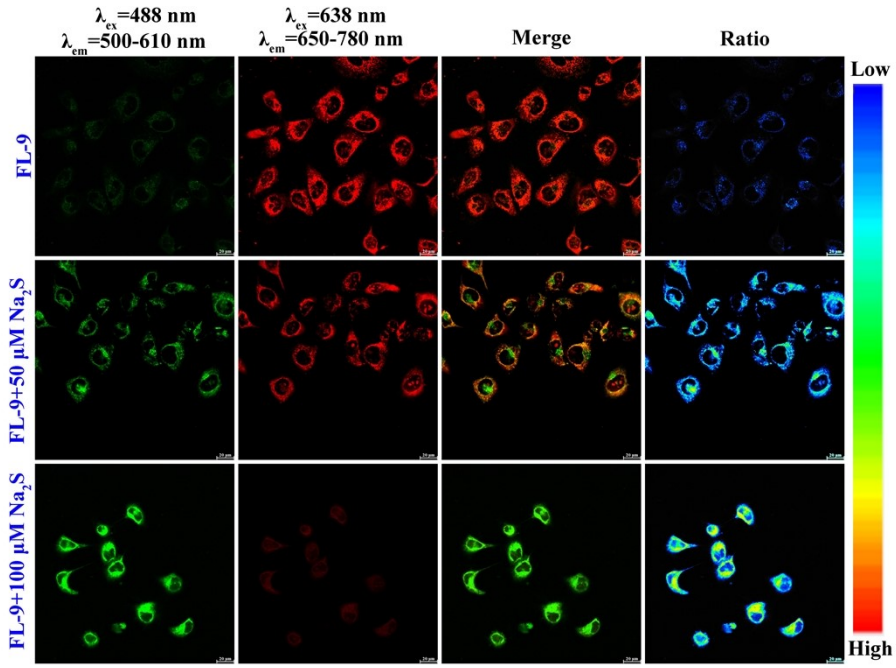

Figure S20 First row, HeLa cells incubated with only **FL-9** (10 μM) for 30 minutes; Second row, the cells pretreated with Na_2S (50 μM) for 30 min and then treated with **FL-9** (10 μM) for 30 minutes; Third row, the cells pretreated with Na_2S (100 μM) for 30 min and then treated with **FL-9** (10 μM) for 30 minutes. The excitation wavelength was 488 nm, the emission collected at 500-610 nm was denoted as the green channel; the excitation wavelength was 638 nm, the emission collected at 650-780 nm was denoted as the green channel. Scale bar = 20μm.

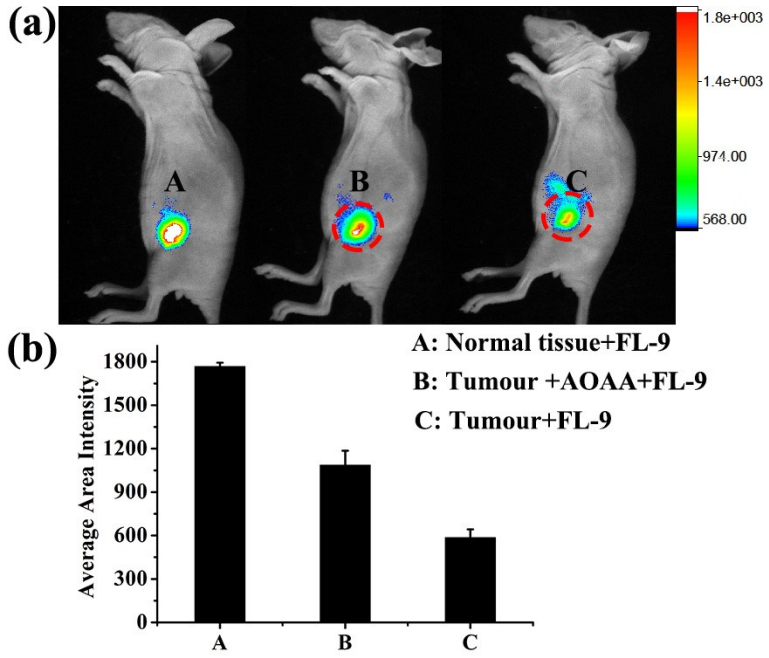

Figure S21 In vivo fluorescence images of H_2S in living mice with **FL-9**. (a) Only saline and saline containing AOAA (400 μM) were injected into normal issue (A) and the tumor tissues (B, C). After 30 min, **FL-9** (20 μM) was injected into the tumor tissues (B, C) and normal issue (A); (b) quantifification of the A, B and C area fluorescence intensity in (a) (n = 3). λ_{ex} = 650 nm, 700 nm emission flter.

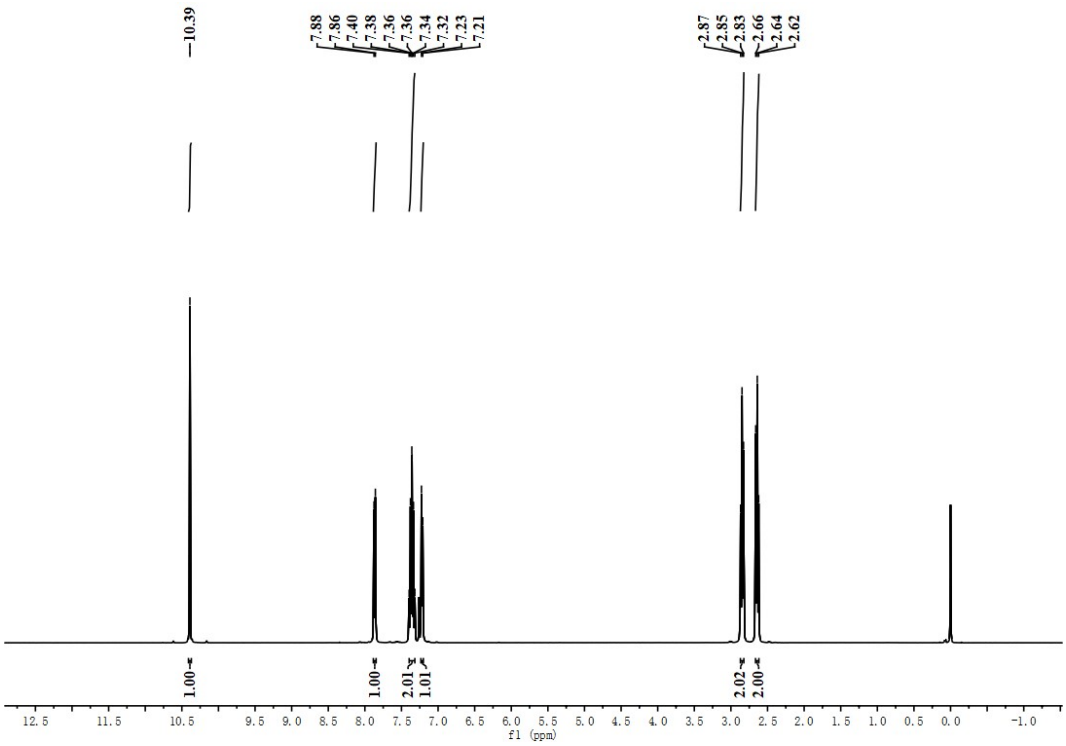

Figure S22 The ^{1}H NMR spectra of **B1**.

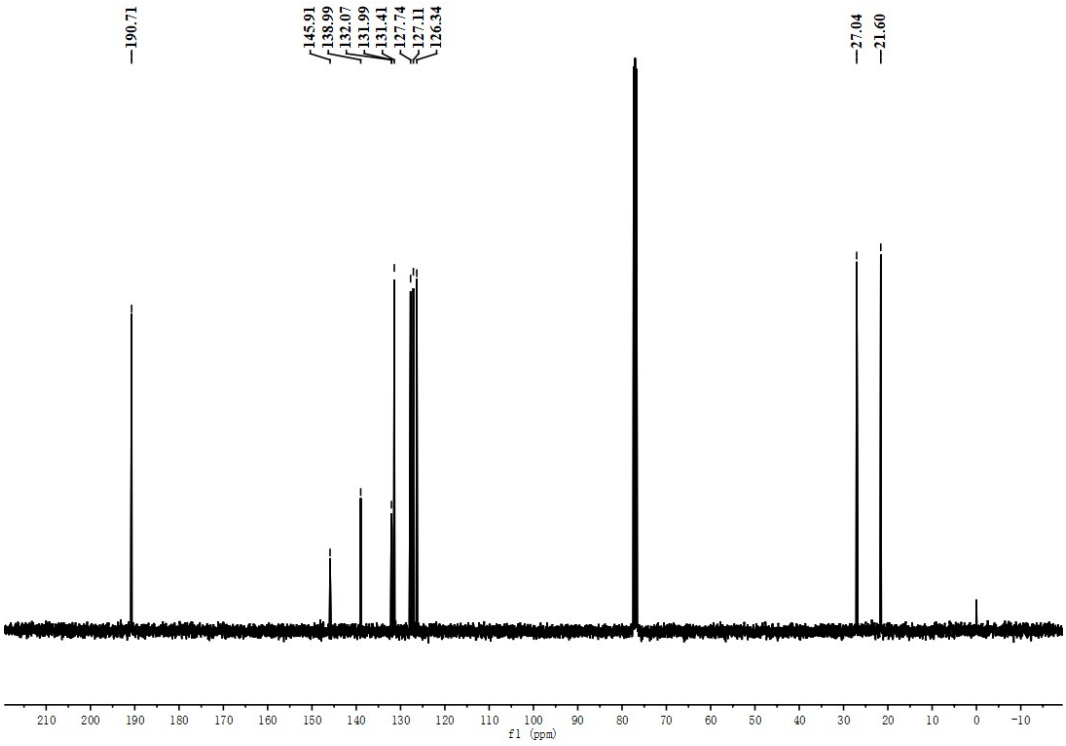

Figure S23 The ^{13}C NMR spectra of **B1**.

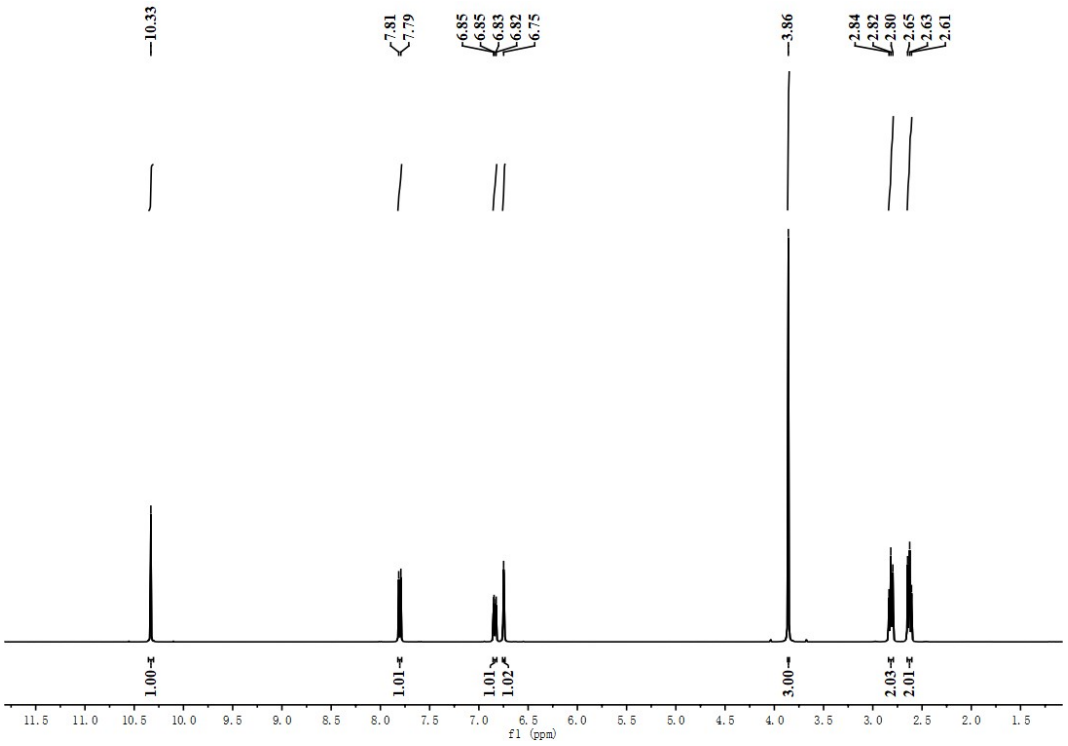

Figure S24 The ^{1}H NMR spectra of **B2**.

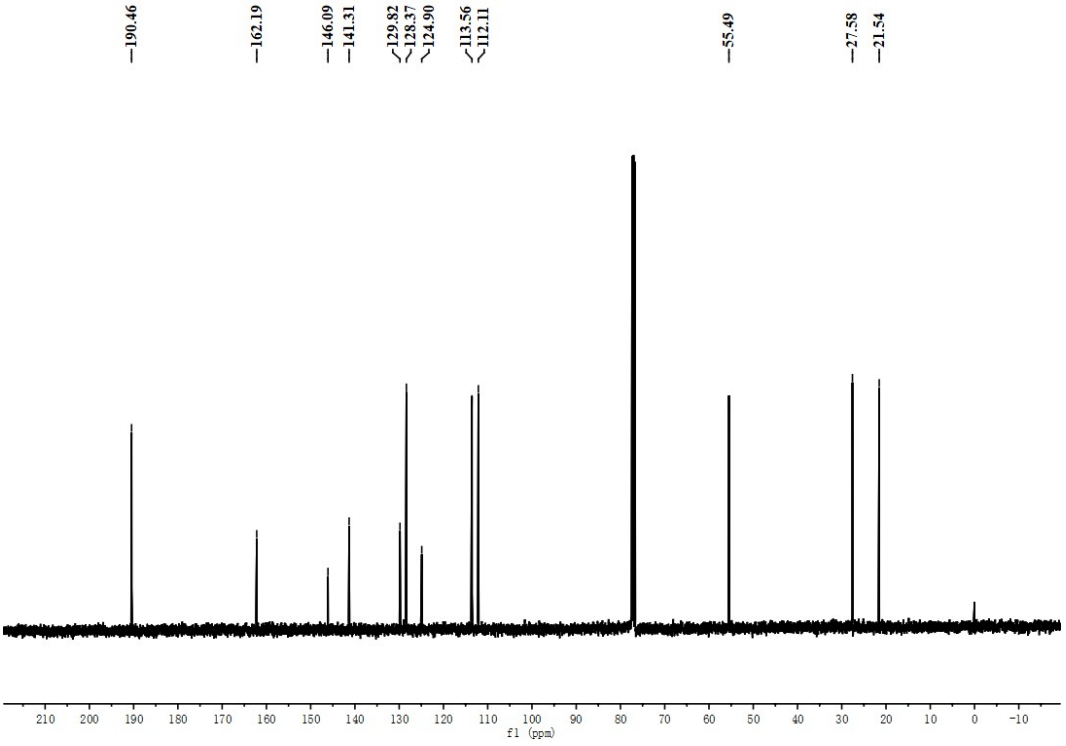

Figure S25 The ^{13}C NMR spectra of **B2**.

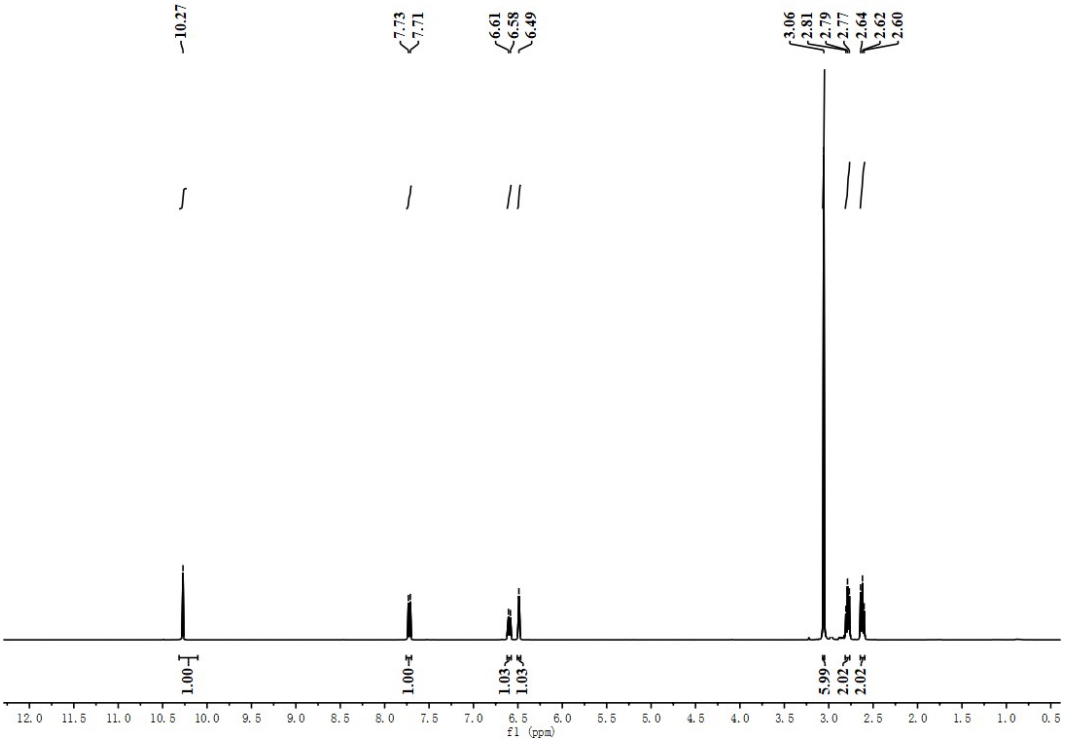

Figure S26 The ^{1}H NMR spectra of **B3**.

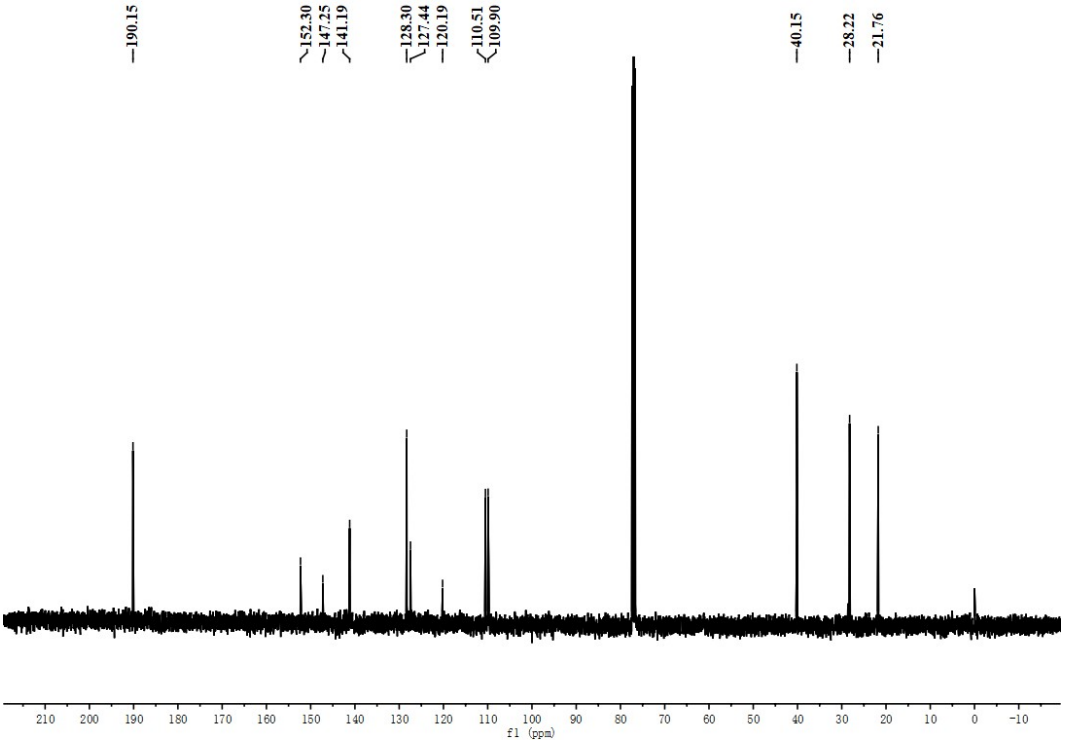

Figure S27 The ^{13}C NMR spectra of **B3**.

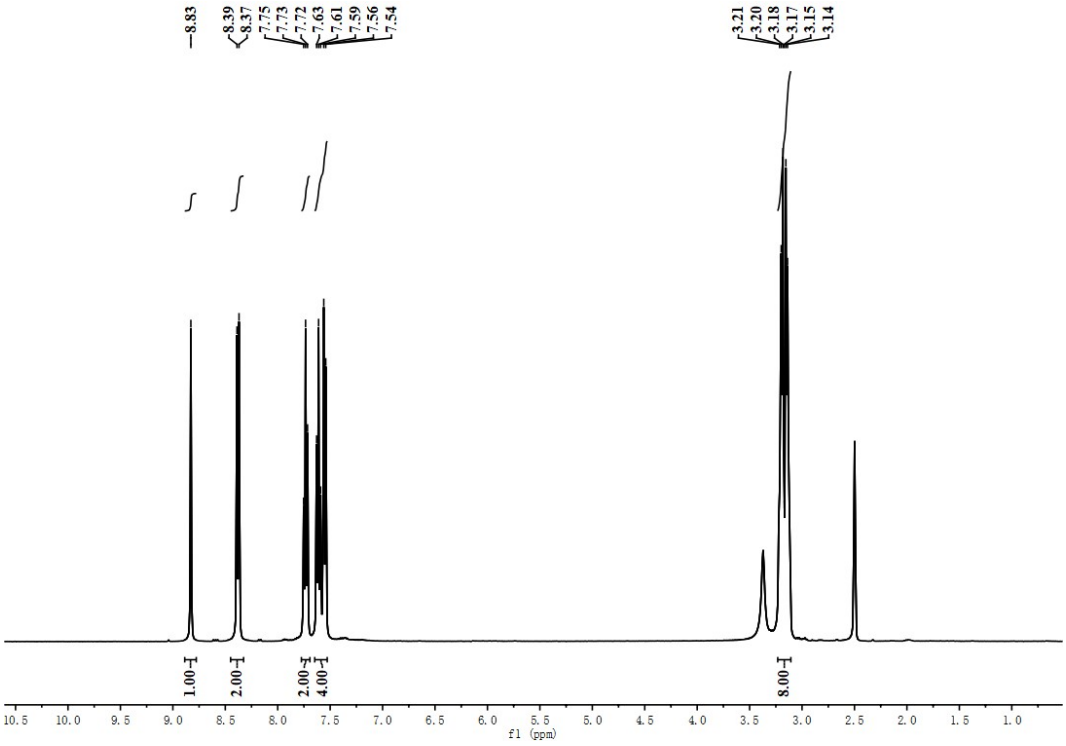

Figure S28 The ^{1}H NMR spectra of **FL-1**.

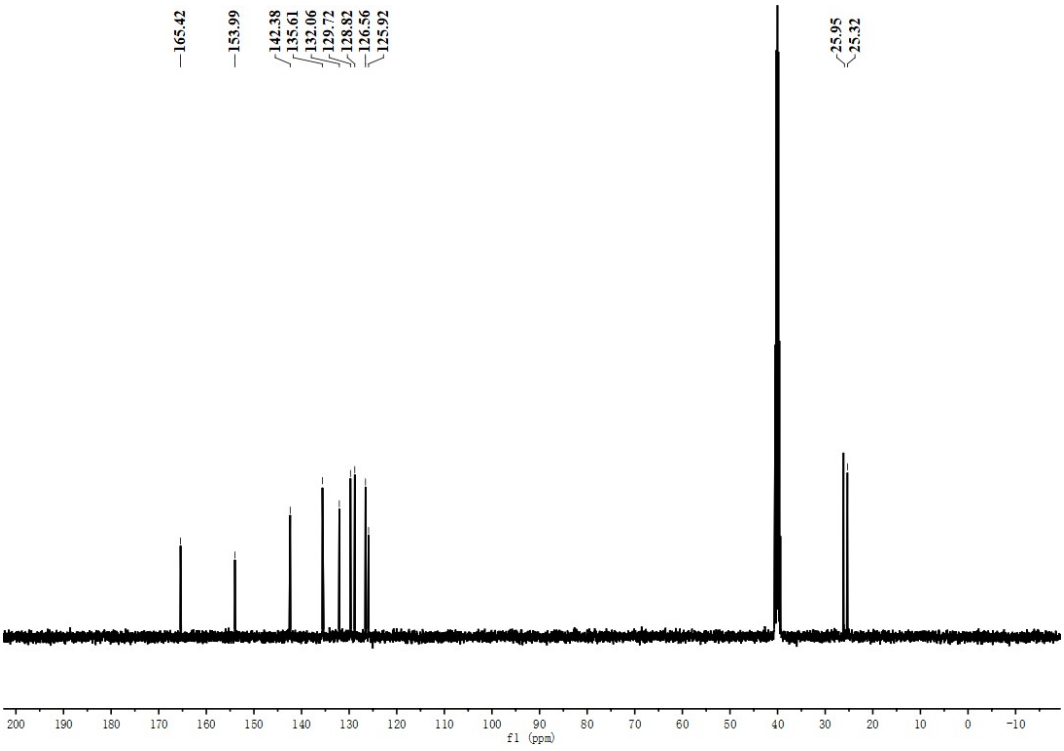

Figure S29 The ^{13}C NMR spectra of **FL-1**.

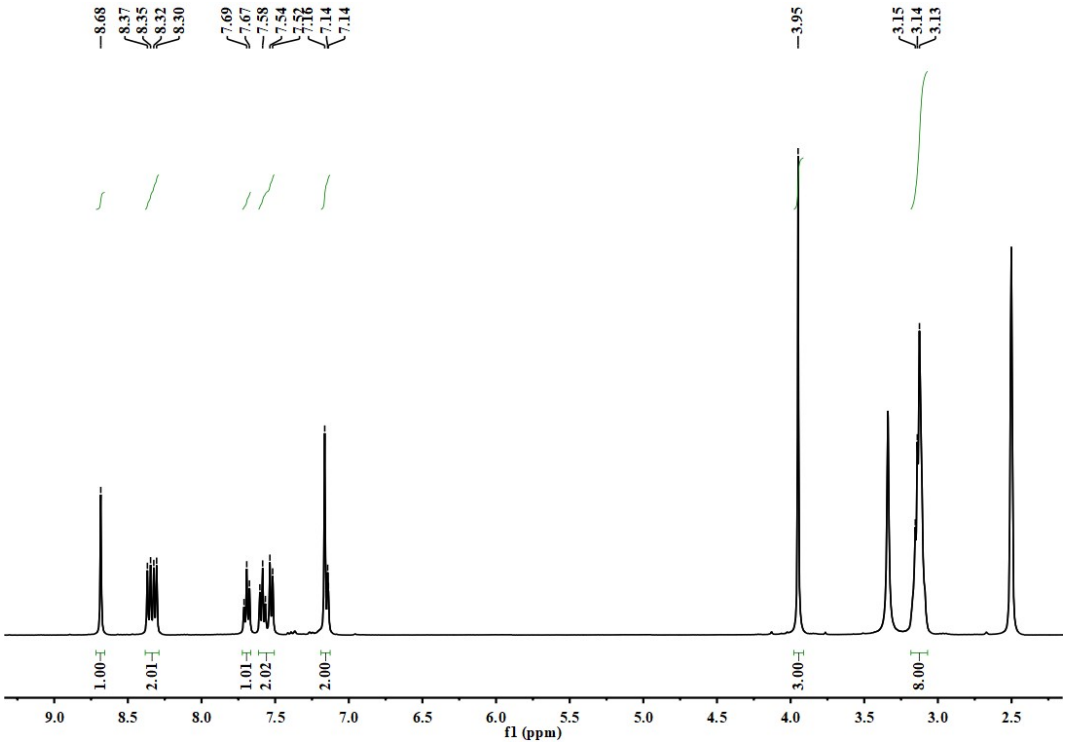

Figure S30 The [1]HNMR spectra of **FL-2**.

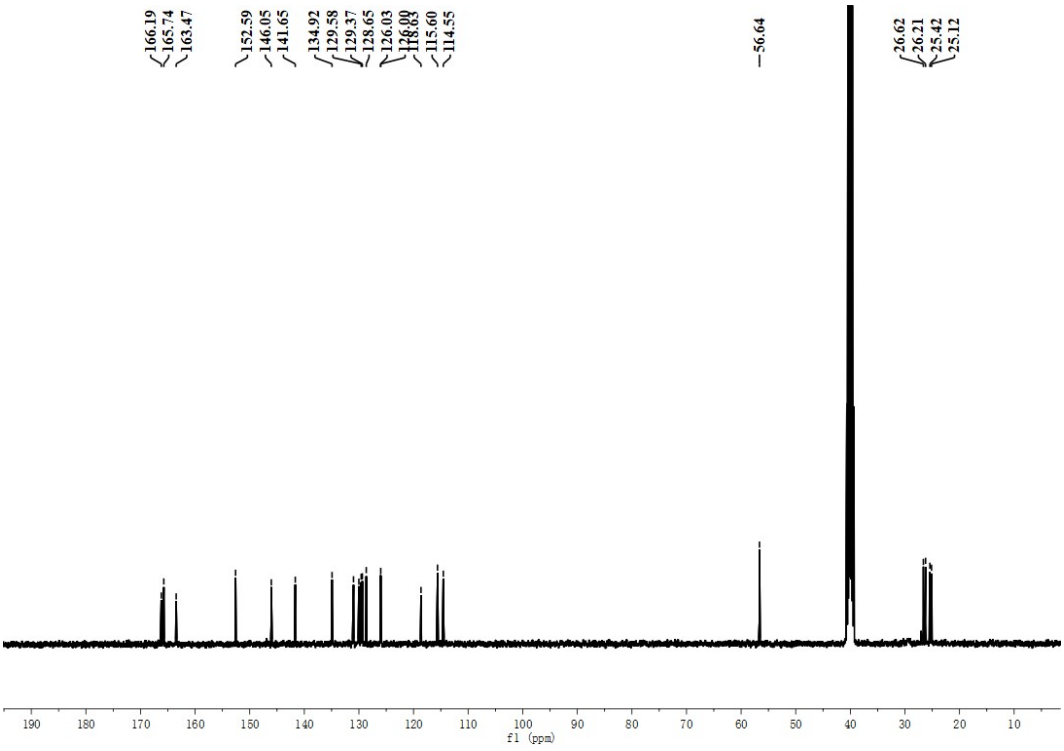

Figure S31 The [13]CNMR spectra of **FL-2**.

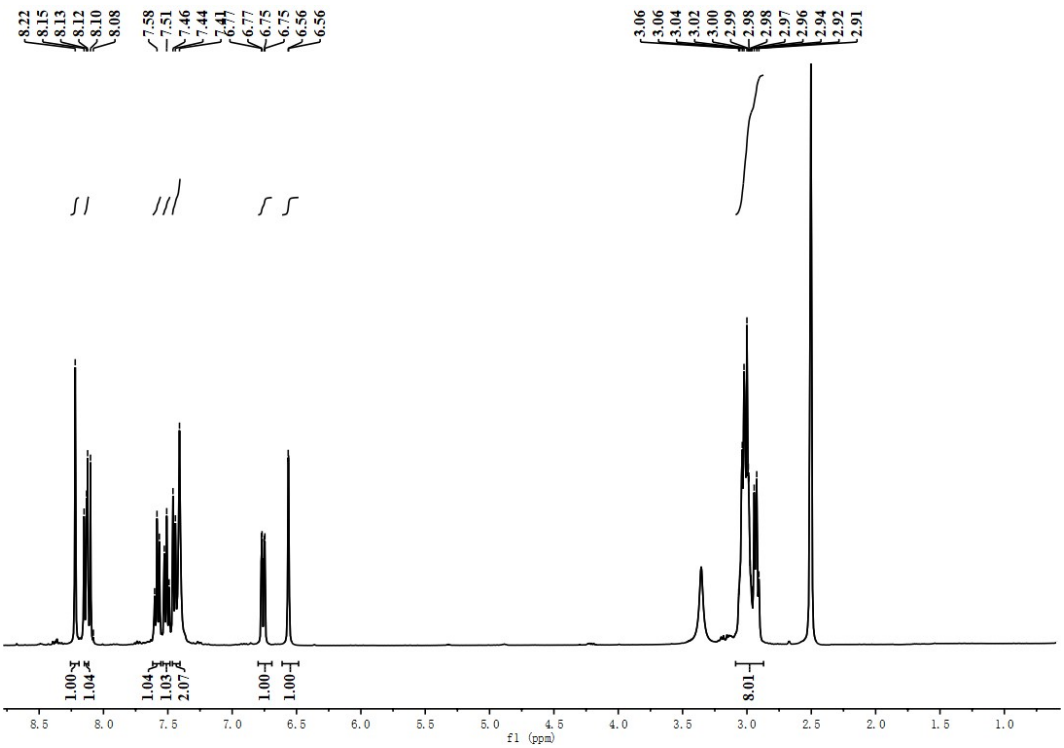

Figure S32 The ^{1}H NMR spectra of **FL-3**.

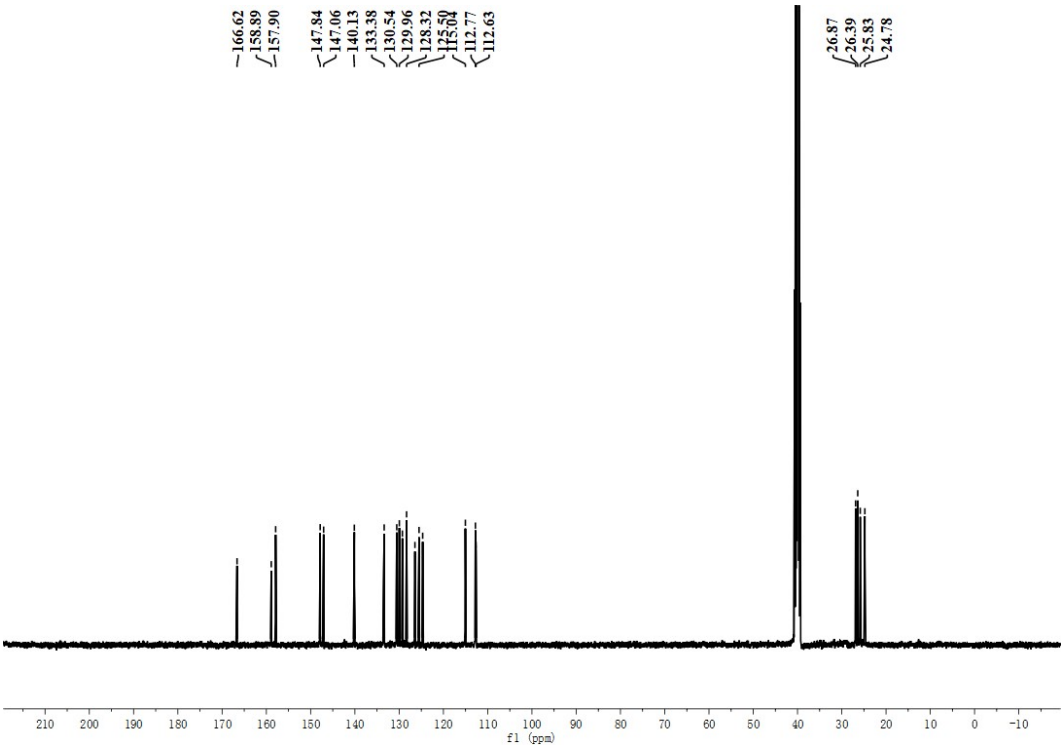

Figure S33 The ^{13}C NMR spectra of **FL-3**.

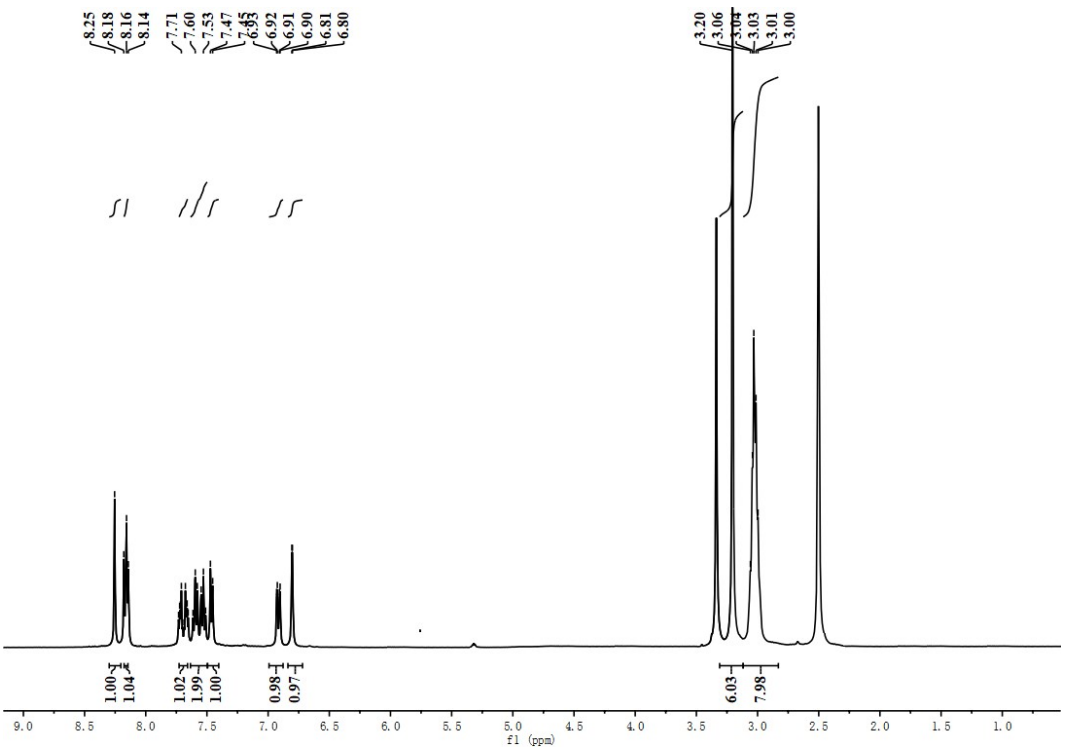

Figure S34 The ^{1}H NMR spectra of **FL-4**.

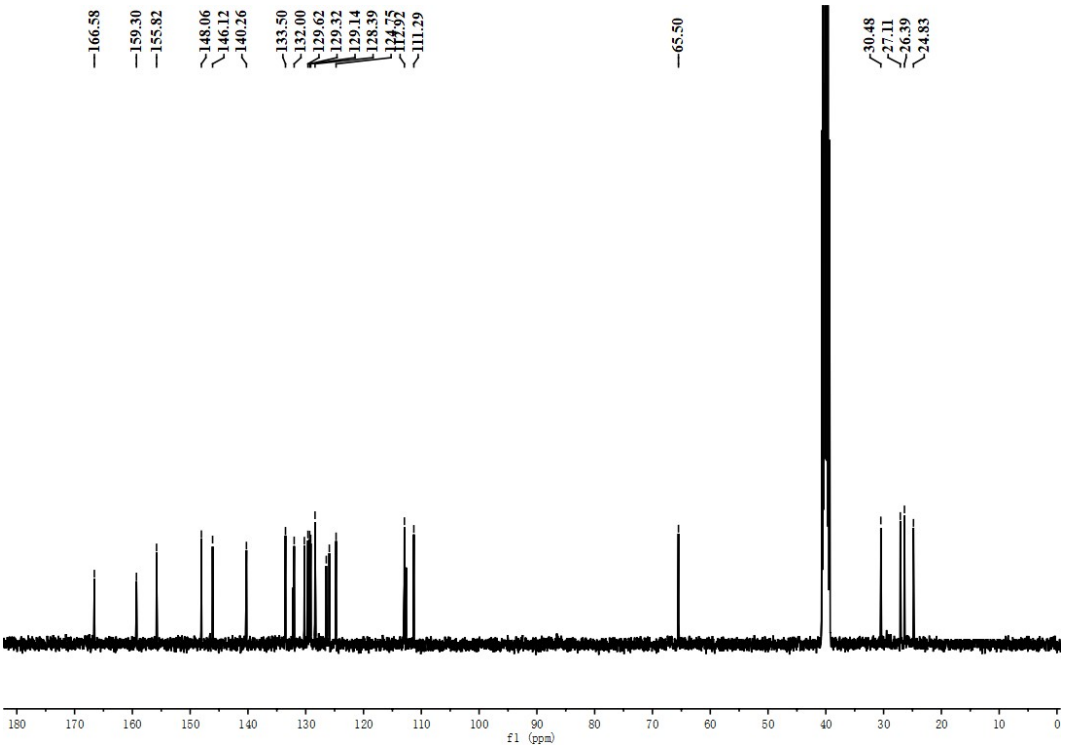

Figure S35 The ^{13}C NMR spectra of **FL-4**.

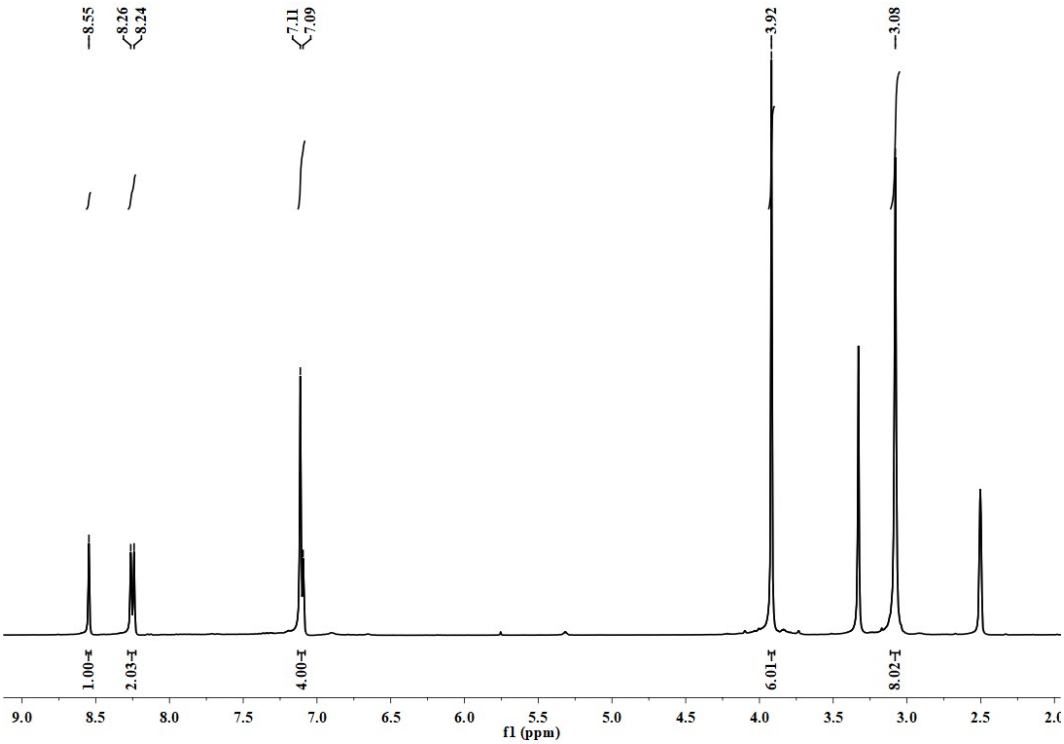

Figure S36 The ^{1}H NMR spectra of **FL-5**.

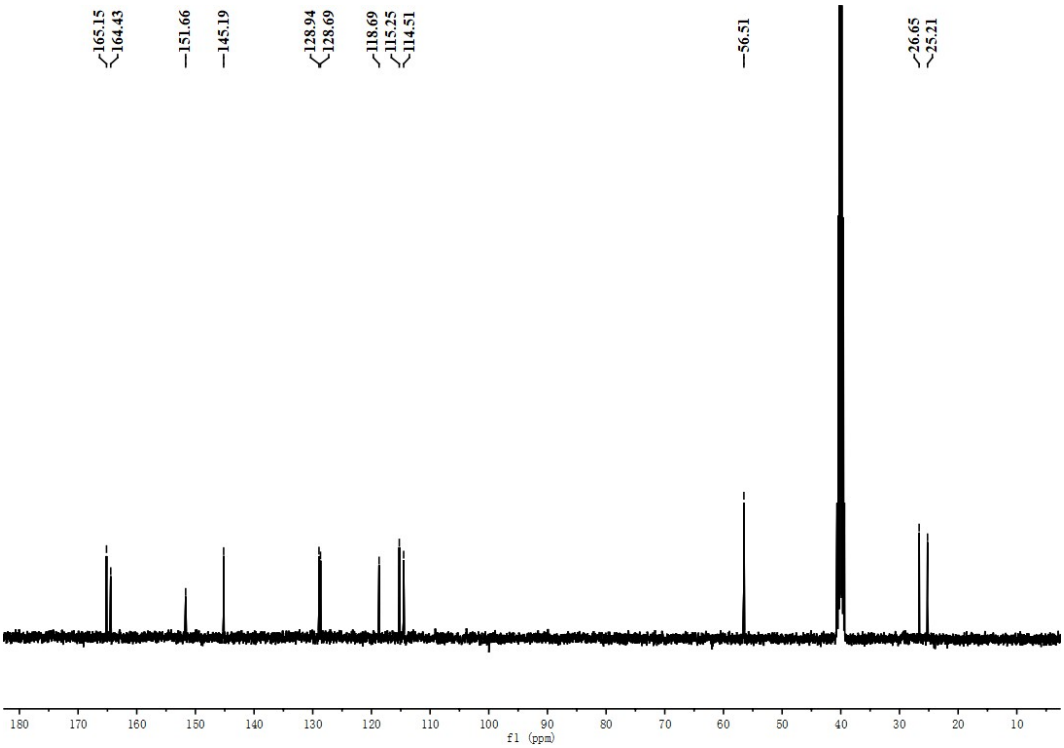

Figure S37 The ^{13}C NMR spectra of **FL-5**.

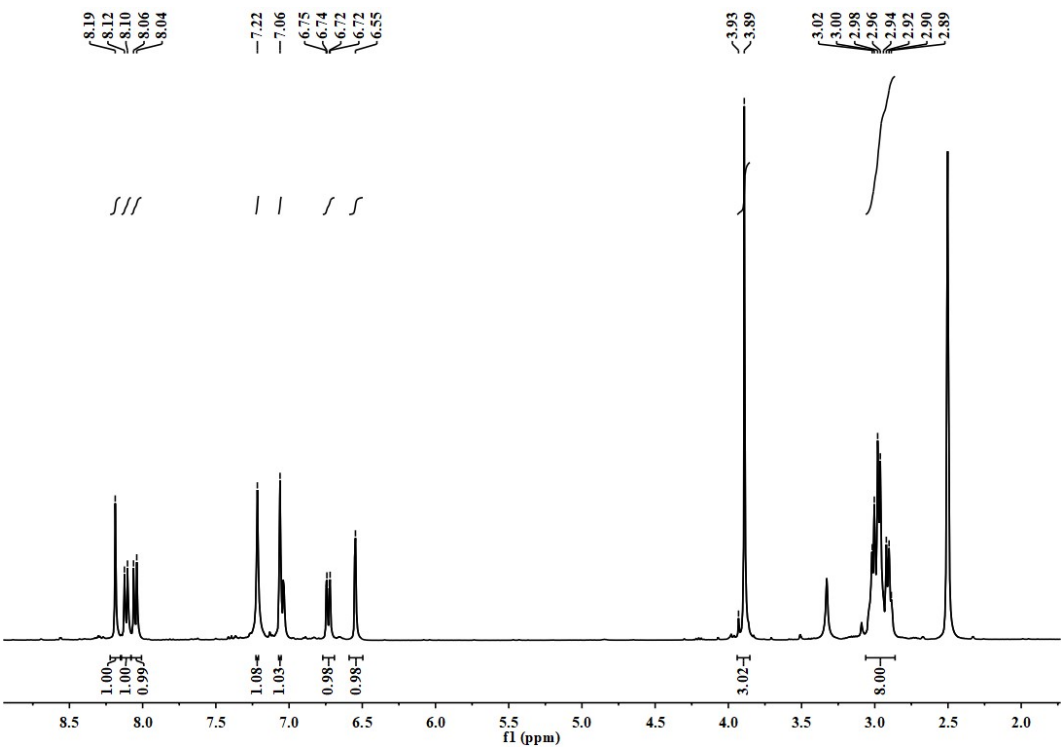

Figure S38 The ^{1}H NMR spectra of **FL-6**.

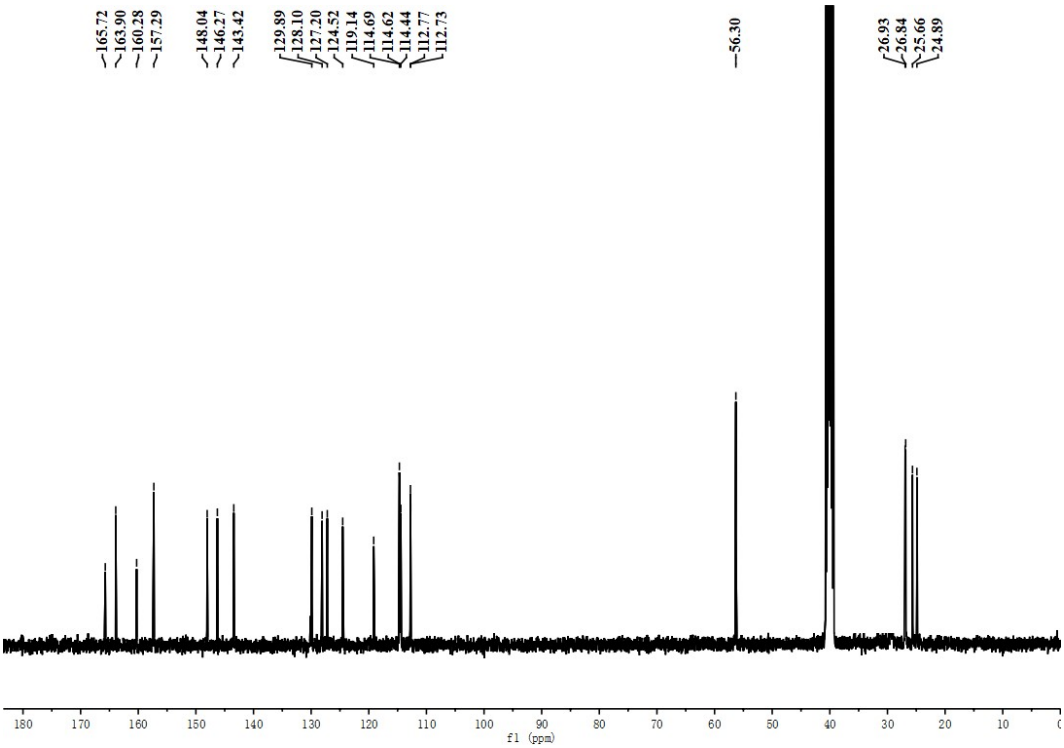

Figure S39 The ^{13}C NMR spectra of **FL-6**.

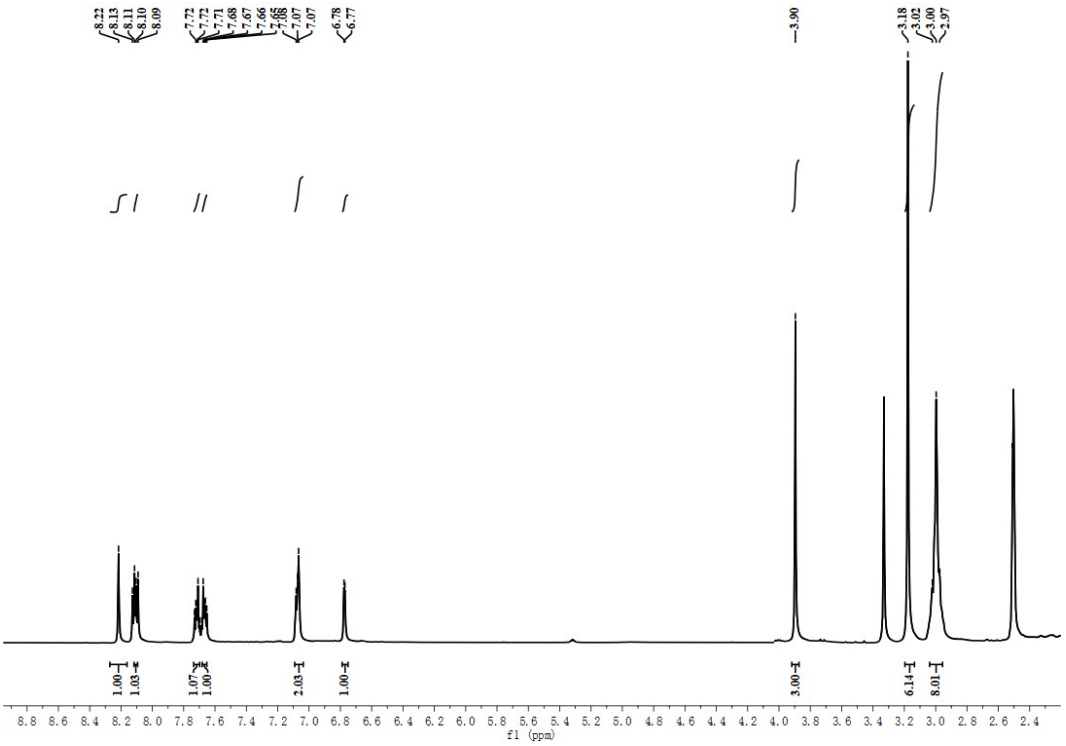

Figure S40 The ^{1}H NMR spectra of **FL-7**.

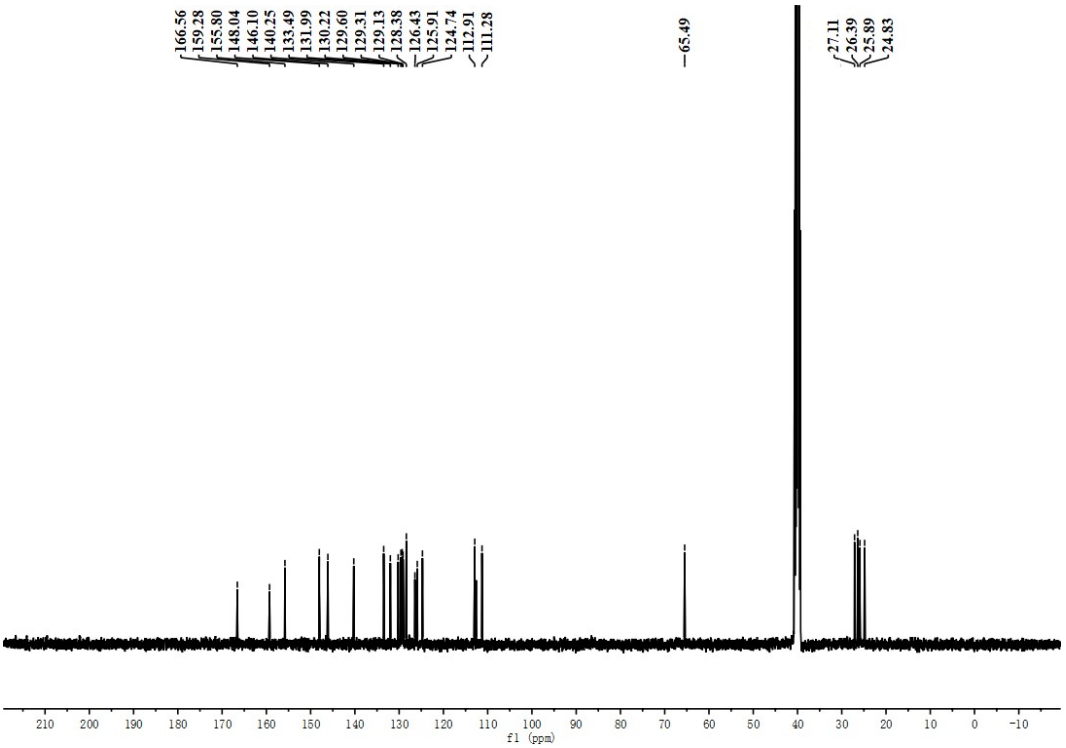

Figure S41 The ^{13}C NMR spectra of **FL-7**.

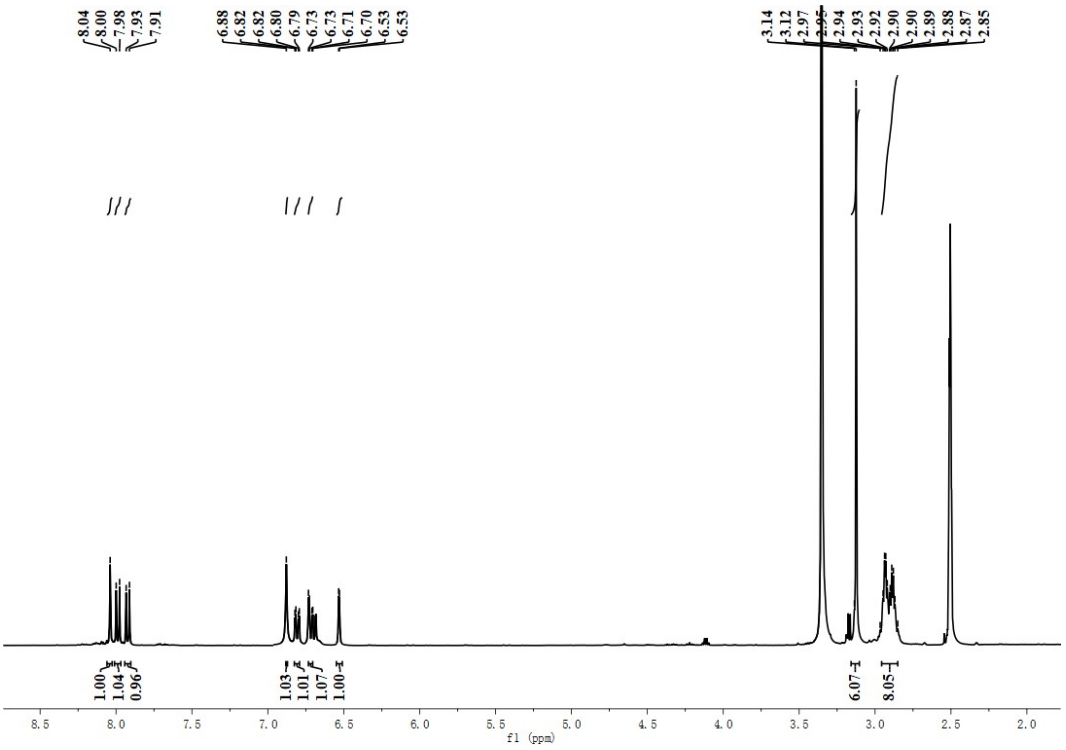

Figure S42 The ^{1}H NMR spectra of **FL-8**.

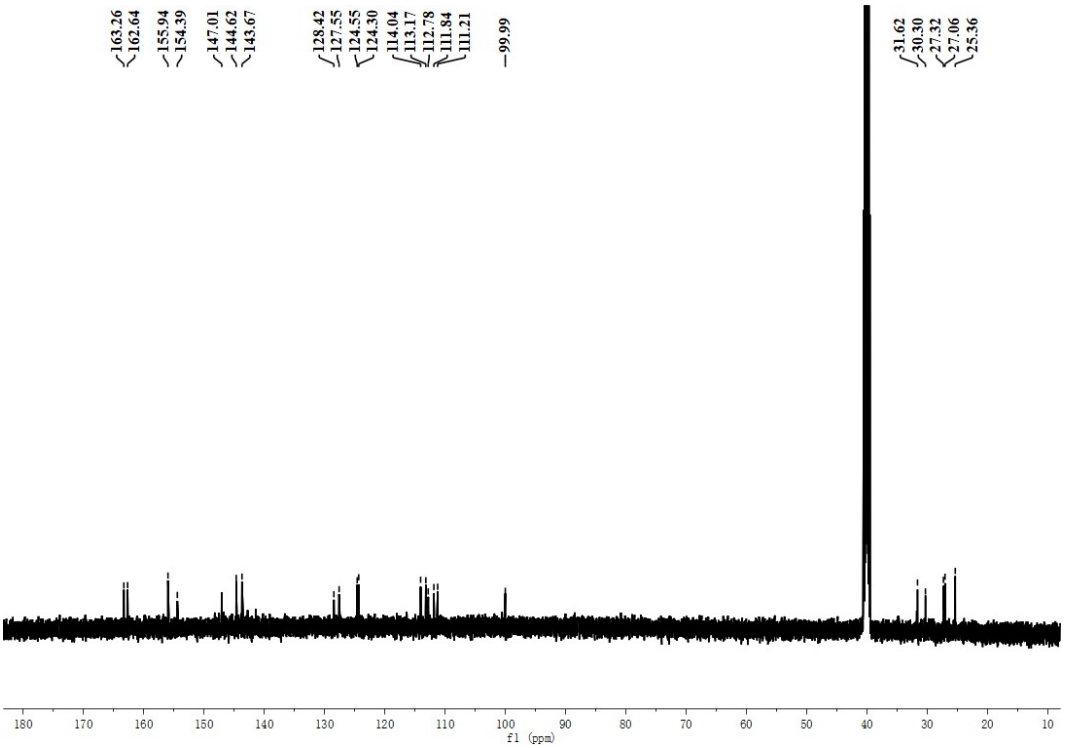

Figure S43 The ^{13}C NMR spectra of **FL-8**.

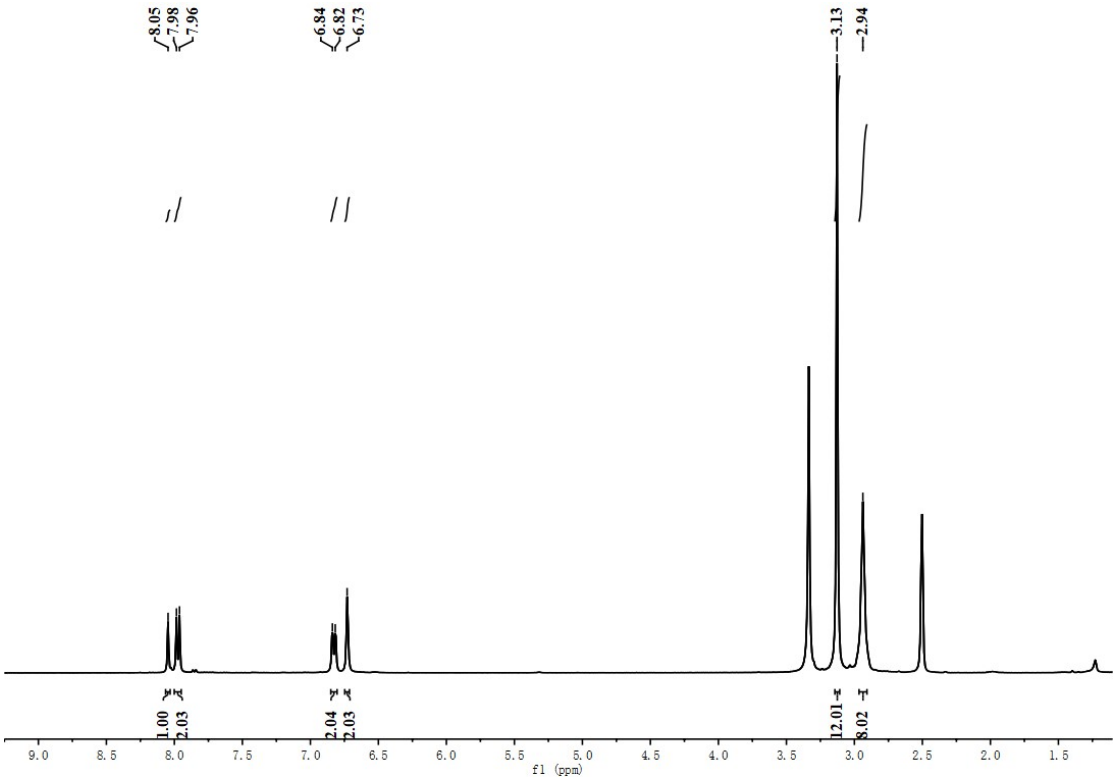

Figure S44 The [1]HNMRspectra of **FL-9**.

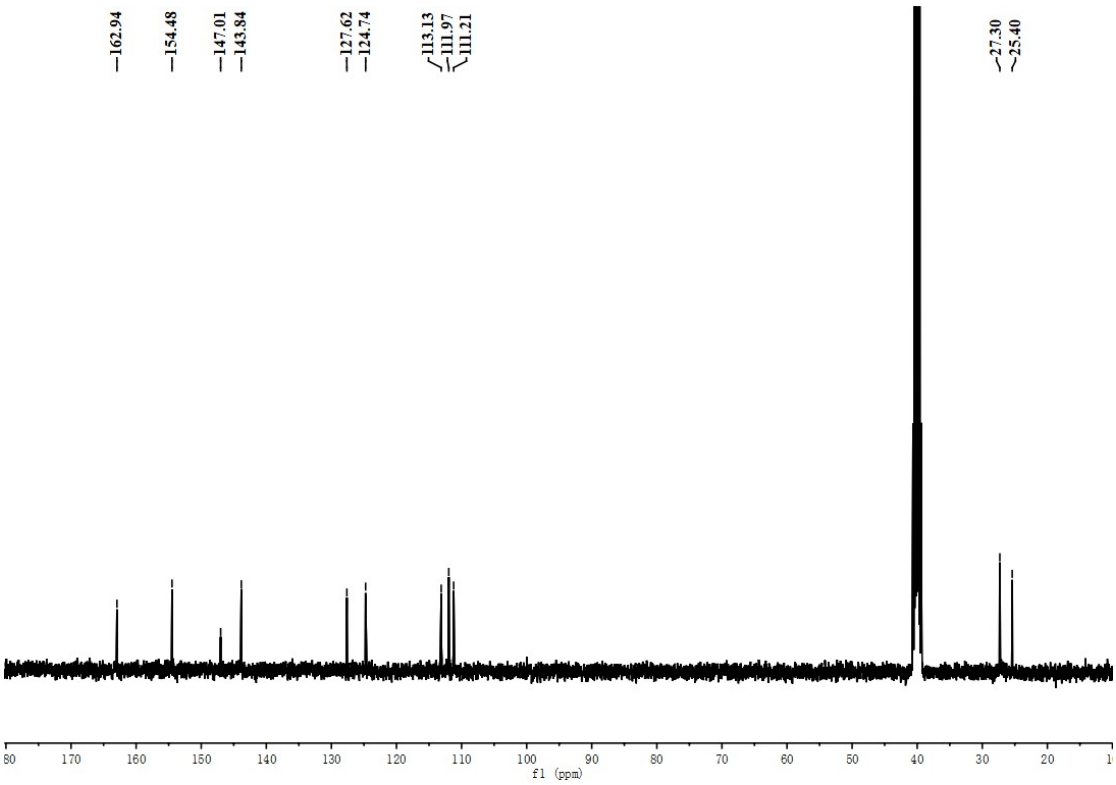

Figure S45 The [13]CNMR spectra of **FL-9**.